ACS Infectious Diseases

Article

Cite This: ACS Infect. Dis. XXXX, XXX, XXX−XXX

pubs.acs.org/journal/aidcbc

Semisynthetic Analogues of Anhydrotetracycline as Inhibitors of Tetracycline Destructase Enzymes

Jana L. Markley,[†] Luting Fang,[†] Andrew J. Gasparrini,[‡] Chanez T. Symister,[†] Hirdesh Kumar,[§] Niraj H. Tolia,[*,§,▽] Gautam Dantas,[*,‡,∥,⊥,#,▽] and Timothy A. Wencewicz[*,†,▽]

[†]Department of Chemistry and [#]Department of Biomedical Engineering, Washington University in St. Louis, One Brookings Drive, St. Louis, Missouri 63130, United States

[‡]The Edison Family Center for Genome Sciences & Systems Biology, Washington University School of Medicine, 4513 Clayton Ave., Campus Box 8510, St. Louis, Missouri 63108, United States

[§]Laboratory of Malaria Immunology and Vaccinology, National Institute of Allergy and Infectious Diseases, National Institutes of Health, 9000 Rockville Pike, BG 29B Rm 4NN08, Bethesda, Maryland 20814, United States

[∥]Department of Pathology and Immunology, Washington University School of Medicine, St. Louis, Missouri 63110, United States

[⊥]Department of Molecular Microbiology, Washington University School of Medicine, 4515 McKinley Avenue, fifth Floor, Room 5314, St. Louis, Missouri 63110, United States

Supporting Information

ABSTRACT: The synthesis and biological evaluation of semisynthetic anhydrotetracycline analogues as small molecule inhibitors of tetracycline-inactivating enzymes are reported. Inhibitor potency was found to vary as a function of enzyme (major) and substrate-inhibitor pair (minor), and anhydrotetracycline analogue stability to enzymatic and nonenzymatic degradation in solution contributes to their ability to rescue tetracycline activity in whole cell *Escherichia coli* expressing tetracycline destructase enzymes. Taken collectively, these results provide the framework for the rational design of next-generation inhibitor libraries en route to a viable and proactive adjuvant approach to combat the enzymatic degradation of tetracycline antibiotics.

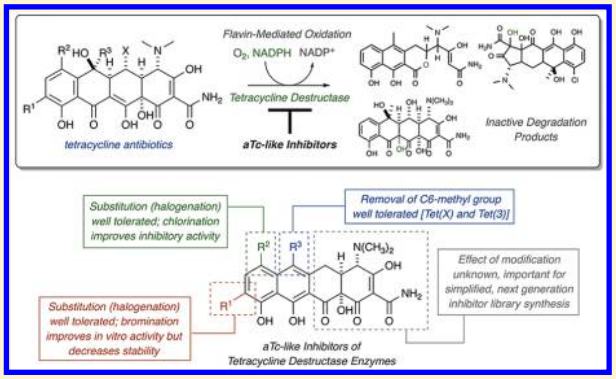

KEYWORDS: *tetracyclines, anhydrotetracycline, tetracycline destructases, Tet(X), antibiotic resistance, inactivating enzymes, enzymology, antibiotic adjuvants, tigecycline, eravacycline, omadacycline*

Since the isolation of chlortetracycline (**2**, aureomycin) from *Streptomyces aureofaciens* in 1948,[1] the tetracycline family of broad-spectrum antibiotics has served as essential medicines for the treatment of bacterial infections in hospital and agricultural settings (Figure 1).[2−8] Driven by challenges with stability, toxicity, and rising antibiotic resistance, the development of more effective, semisynthetic tetracycline variants has led to the introduction of next-generation tetracycline antibiotics tailored to overcome emerging resistance mechanisms.[9−12] In this regard, the majority of current treatment strategies employ the use of second-generation C6-deoxy-tetracyclines (i.e., doxycycline and minocycline), which were developed to overcome efflux and stability issues,[9] and third-generation glycylcyclines (tigecycline,[13,14] eravacycline,[15,16] and omadacycline[17]), which were designed to evade efflux and ribosomal protection[9,18] and are used as last-resort treatments for multidrug resistant infections (Figure 1).[19−21] While the most common, clinically relevant resistance mechanisms for tetracycline antibiotics include efflux and ribosomal protection,[9,22,23] those mechanisms that facilitate intra- and extra-cellular antibiotic clearance—often through the enzymatic, irreversible inactivation of antibiotic scaffolds—frequently pervade resistance landscapes as the most efficient means of achieving resistance.[24,25] Historically, the enzymatic inactivation of β-lactam antibiotics has been well-studied,[26−28] and strategies aimed at combatting this resistance using an adjuvant approach—where the antibiotic is coadministered with a small molecule inhibitor of the inactivating enzyme—have emerged as fundamentally useful tools for the rescue of β-lactam antibiotics in the clinic.[29−32] With the discovery and characterization of 10 tetracycline-inactivating enzymes with varying resistance profiles,[33,34] the development of small molecule inhibitors of tetracycline destructase enzymes stands at the forefront of strategies aimed at combatting the imminent clinical emergence of this resistance mechanism in multidrug resistant infections. We herein report preliminary findings focused on understanding

Received: December 9, 2018

DOI: 10.1021/acsinfecdis.8b00349
ACS Infect. Dis. XXXX, XXX, XXX−XXX

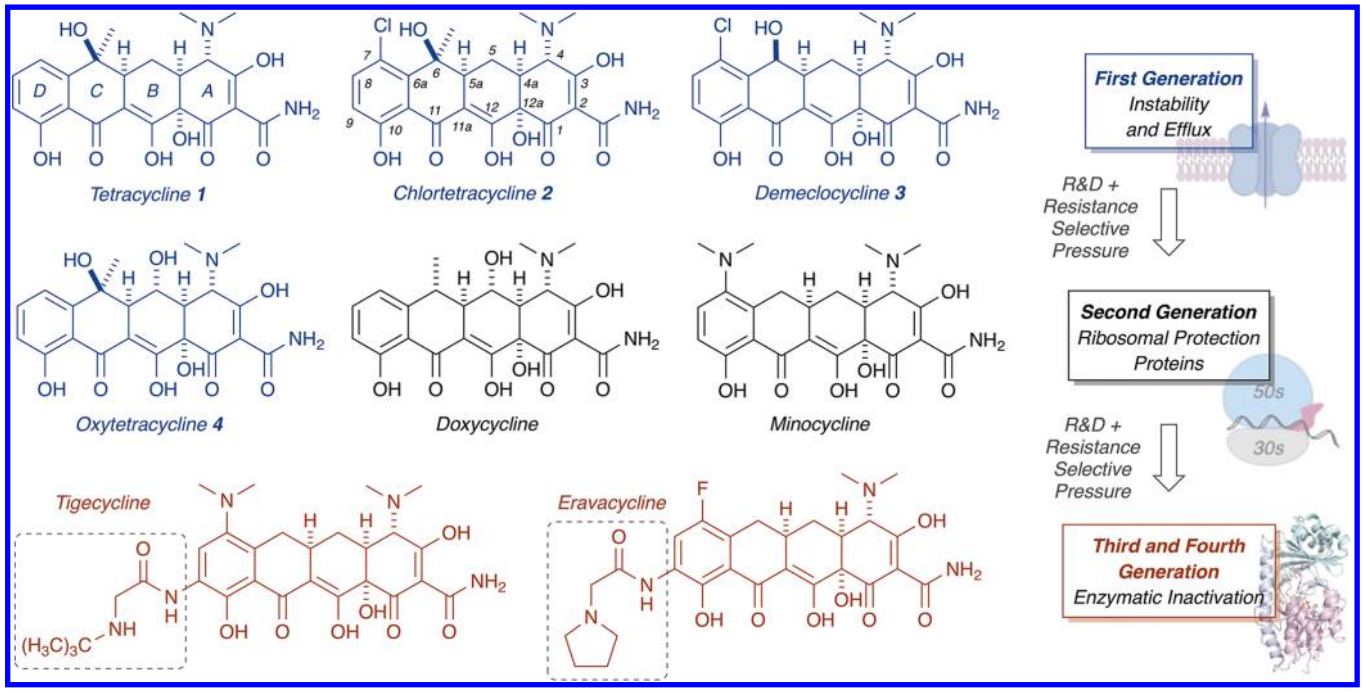

Figure 1. Tetracycline development and parallel emergence of resistance mechanisms.

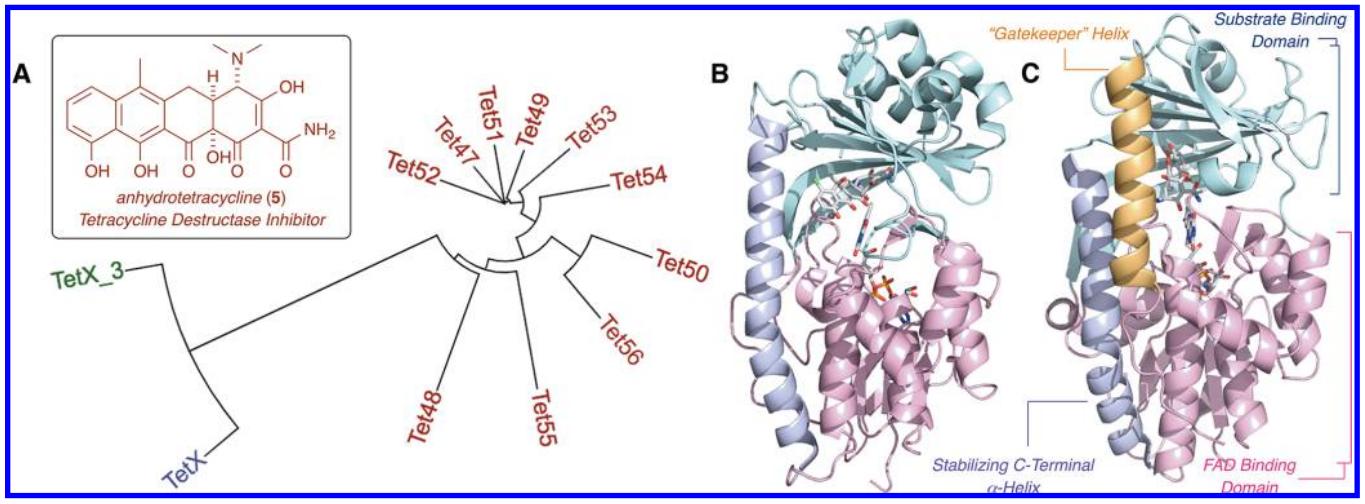

Figure 2. Introduction to the tetracycline destructase family of FMO enzymes and structure of the first inhibitor, anhydrotetracycline (**5**). (A) Phylogenetic tree [aligned with Clustal Omega and viewed using iTOL software]. (B) X-ray crystal structure of chlortetracycline bound to Tet(X) (PDB ID 2y6r). (C) X-ray crystal structure of chlortetracycline bound to Tet(50) (PDB ID 5tui).

the factors that influence inhibitor potency and stability en route to the development of viable adjuvant approaches to counter tetracycline resistance by enzymatic inactivation.

Tetracycline-inactivating enzymes, including the most studied tetracycline destructase, Tet(X),[33] and the subsequently identified enzymes Tet(47)−Tet(56),[34] are Class A flavin-dependent monooxygenase enzymes confirmed to confer tetracycline resistance by the nonreversible functionalization of the tetracycline scaffolds (Figure 2A). Gut-derived Tet(X) and soil-derived Tet(47)−Tet(56) possess unique three-dimensional (3D) structures, which directly contribute to the observed variation in phenotypic tetracycline resistance profiles across enzyme clades (Figure 2B,C).[35−37] In general, tetracycline destructase enzymes are composed of at least three functional domains: a substrate-binding domain, a flavin adenine dinucleotide (FAD)-binding domain, and a C-terminal α helix that stabilizes the association of the two. The presence of a second C-terminal α helix, termed the "Gatekeeper" helix, was also observed for the soil-derived tetracycline destructases [Tet(47)−Tet(56)] and is thought to facilitate substrate recognition and binding.[37]

A variety of substrate binding modes have been observed for Tet(X) and the tetracycline destructases. A search for competitive inhibitors identified anhydrotetracycline (aTC, **5**), a tetracycline biosynthetic precursor, as a potential broad-spectrum inhibitor (Figures 1, 2).[37] aTC showed dose-dependent and potent inhibition of tetracycline destructases *in vitro* and rescued tetracycline antibiotic activity against *Escherichia coli* overexpressing the resistance enzymes on an inducible plasmid. The crystal structure of aTC bound to Tet50 revealed a novel inhibitor binding mode that pushes the FAD cofactor out of the active site to stabilize an inactive

DOI: 10.1021/acsinfecdis.8b00349
ACS Infect. Dis. XXXX, XXX, XXX−XXX

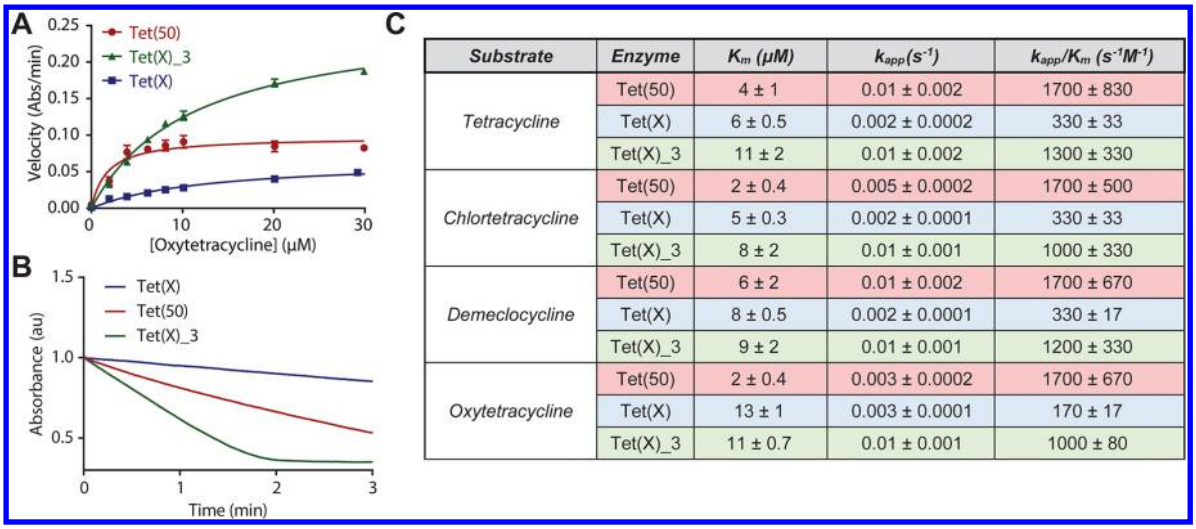

C

Substrate	Enzyme	K_m (μM)	k_{app} (s^{-1})	k_{app}/K_m ($s^{-1}M^{-1}$)
Tetracycline	Tet(50)	4 ± 1	0.01 ± 0.002	1700 ± 830
	Tet(X)	6 ± 0.5	0.002 ± 0.0002	330 ± 33
	Tet(X)_3	11 ± 2	0.01 ± 0.002	1300 ± 330
Chlortetracycline	Tet(50)	2 ± 0.4	0.005 ± 0.0002	1700 ± 500
	Tet(X)	5 ± 0.3	0.002 ± 0.0001	330 ± 33
	Tet(X)_3	8 ± 2	0.01 ± 0.001	1000 ± 330
Demeclocycline	Tet(50)	6 ± 2	0.01 ± 0.002	1700 ± 670
	Tet(X)	8 ± 0.5	0.002 ± 0.0001	330 ± 17
	Tet(X)_3	9 ± 2	0.01 ± 0.001	1200 ± 330
Oxytetracycline	Tet(50)	2 ± 0.4	0.003 ± 0.0002	1700 ± 670
	Tet(X)	13 ± 1	0.003 ± 0.0001	170 ± 17
	Tet(X)_3	11 ± 0.7	0.01 ± 0.001	1000 ± 80

Figure 3. Michaelis–Menten kinetics of tetracycline destructase degradation of first generation tetracyclines. (A) Representative Michaelis–Menten plot of tetracycline destructase degradation of oxytetracycline. (B) Representative optical absorbance kinetic plots for the degradation of oxytetracycline by tetracycline destructase enzymes [as observed at 400 nm for Tet(50) and Tet(X)_3; 380 nm for Tet(X)]. (C) Apparent K_m, k_{app}, and catalytic efficiencies for the tetracycline destructase-mediated degradation of tetracycline, chlortetracycline, demeclocycline, and oxytetracycline. Error bars represent standard deviation for two independent trials.

enzyme conformation.[37] Upon the basis of these preliminary results, we crafted two hypotheses with regard to tetracycline destructase inhibition. Because of the variability observed in phenotypic resistance profiles between tetracycline destructase enzymes and phylogenetic clades, we hypothesized that inhibitor potency would also vary as a function of enzyme and inhibitor-substrate pairing; thus, a library of inhibitors may be required to preserve the viability and effectiveness of an adjuvant approach. This has proven to be the case with β-lactam adjuvants, where multiple generations of inhibitors are required to cover the diverse families of β-lactamase resistance enzymes (classes A–D) present in the clinic.[29] In addition, we proposed that aTC, in particular, could serve as a privileged scaffold about which to design inhibitor libraries. Thus, we herein report the generation and biological evaluation of four semisynthetic derivatives of anhydrotetracycline as potential inhibitors of tetracycline destructase enzymes. To identify the factors affecting the inhibition of tetracycline-inactivating enzymes, we assessed the inhibitory activity of the aTC analogue library, in reference to aTC, against the degradation of first-generation tetracyclines by three representative tetracycline destructase enzymes (Figure 1). Taken collectively, these results highlight the factors that influence inhibitor potency and stability and provide the framework for the rational design of next-generation inhibitor libraries.

RESULTS AND DISCUSSION

Michaelis–Menten Kinetics Highlight Enzyme Differences. Three representative tetracycline destructase enzymes were chosen based upon observed phenotypic resistance profiles and phylogenetic clustering.[34] These enzymes—soil-derived Tet(50) and gut-derived Tet(X) and Tet(X)_3 [GenBank KU547176.1]—were recombinantly expressed and purified from BL21-Star (DE3) competent *E. coli*. For each enzyme, the *in vitro* enzyme-dependent inactivation of first-generation tetracyclines was characterized using an optical absorbance kinetic assay developed in our laboratory.[34,37] Apparent Michaelis–Menten kinetic parameters were determined from the enzyme- and time-dependent degradation of tetracycline (**1**), chlortetracycline (**2**), demeclocycline (**3**), and oxytetracycline (**4**). Representative Michaelis–Menten plots for the enzymatic degradation of oxytetracycline are shown in Figure 3A.

Consistent with previous reports,[37] micromolar (μM) apparent binding affinities (K_m), ranging from 2 μM to 13 μM, were observed across all enzyme–substrate combinations (Figure 3). Apparent rate (k_{app}) of tetracycline degradation was highest for Tet(X)_3, followed closely by Tet(50), and last by Tet(X); this variation in apparent rate is highlighted in the deviation in shape and slope of the raw plots of enzyme-dependent tetracycline degradation, observed as the change in the absorbance at 400 nm over time (Figure 3B). Conversely, apparent catalytic efficiency (k_{app}/K_m) was highest for Tet(50) over Tet(X)_3—due to a 2–10 fold difference in apparent K_m. This trend is consistent with the hypothesis that Gatekeeper helix-facilitated substrate recognition results in an increase in substrate specificity and turnover for the soil-derived tetracycline destructases (Figure 2).[37] The second, C-terminal gatekeeper helix is notably absent in X-ray crystal structures of gut-derived, canonical tetracycline-inactivating enzyme, Tet(X) (Figure 2),[35] and the presence or absence of a similar helix in Tet(X)_3—which clusters closely with Tet(X)—is currently unknown. Similar apparent binding affinities (K_m) were observed for phylogenetically clustered Tet(X)_3 and Tet(X), though five- to eight-fold differences in apparent rate results in drastically different catalytic efficiencies for the two gut-derived enzymes (Figure 3C). The paradoxical functional similarities of Tet(X)_3 to both Tet(50) in apparent rate and Tet(X) in binding affinity and resistance phenotype, *vide infra*, has garnered interest in the unique facets of its three-dimensional structure that allows for accelerated turnover and broad substrate scope; efforts to resolve an X-ray crystal structure of Tet(X)_3 are currently ongoing in our laboratories and will be reported in due course. Taken collectively, the variability in binding affinity and catalytic efficiency highlights both enzyme-to-enzyme and substrate-to-substrate differences across the tetracycline destructase family of enzymes. In this light, we hypothesized this same variability would manifest in inhibitor

DOI: 10.1021/acsinfecdis.8b00349
ACS Infect. Dis. XXXX, XXX, XXX–XXX

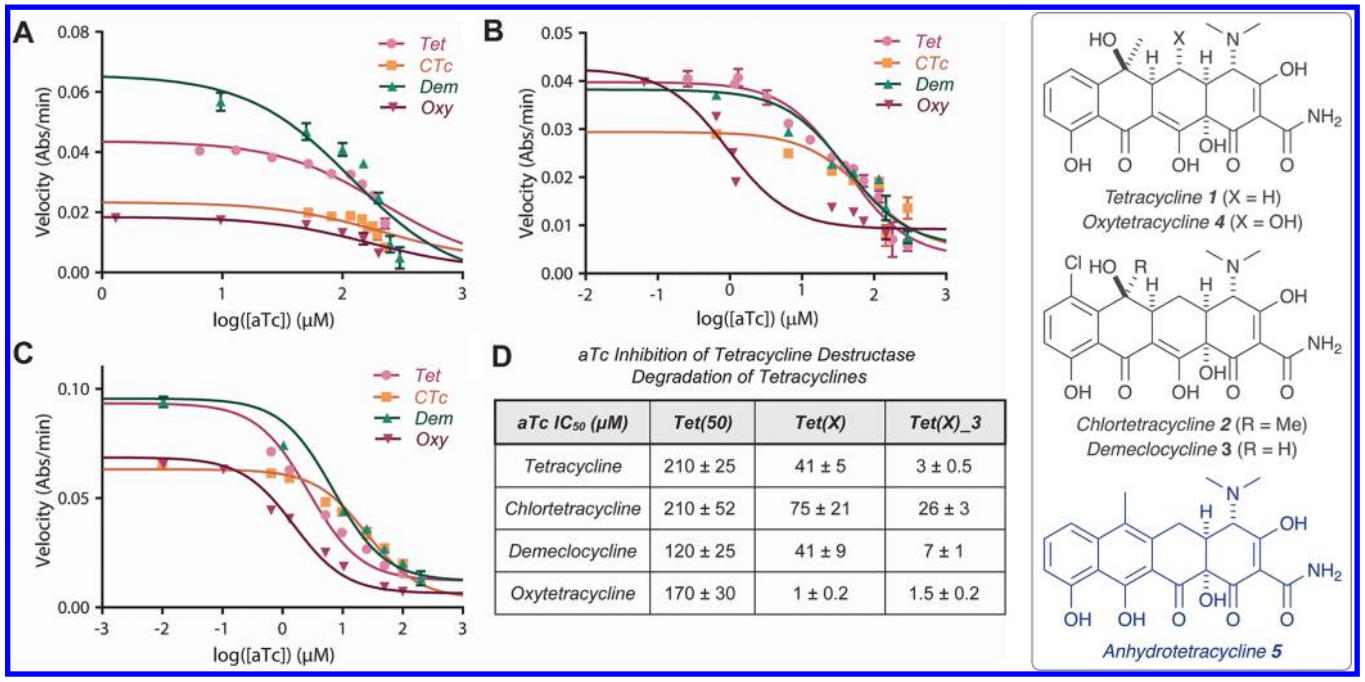

aTc IC_{50} (μM)	Tet(50)	Tet(X)	Tet(X)_3
Tetracycline	210 ± 25	41 ± 5	3 ± 0.5
Chlortetracycline	210 ± 52	75 ± 21	26 ± 3
Demeclocycline	120 ± 25	41 ± 9	7 ± 1
Oxytetracycline	170 ± 30	1 ± 0.2	1.5 ± 0.2

Figure 4. *In vitro* aTC inhibition of tetracycline destructase degradation of first-generation tetracycline antibiotics as observed via an optical absorbance kinetic assay. (A) aTc inhibition of Tet(50) degradation of tetracyclines. (B) aTc inhibition of Tet(X) degradation of tetracyclines. (C) aTc inhibition of Tet(X)_3 degradation of tetracyclines. (D) Apparent IC_{50} for aTC inhibition (denoted for each substrate and enzyme). Error bars represent standard deviation for three independent trials. All data points possess error bars, though some are not visible at the plotted scale.

Scheme 1. Semisynthetic Strategies toward aTC Analogues 6−9

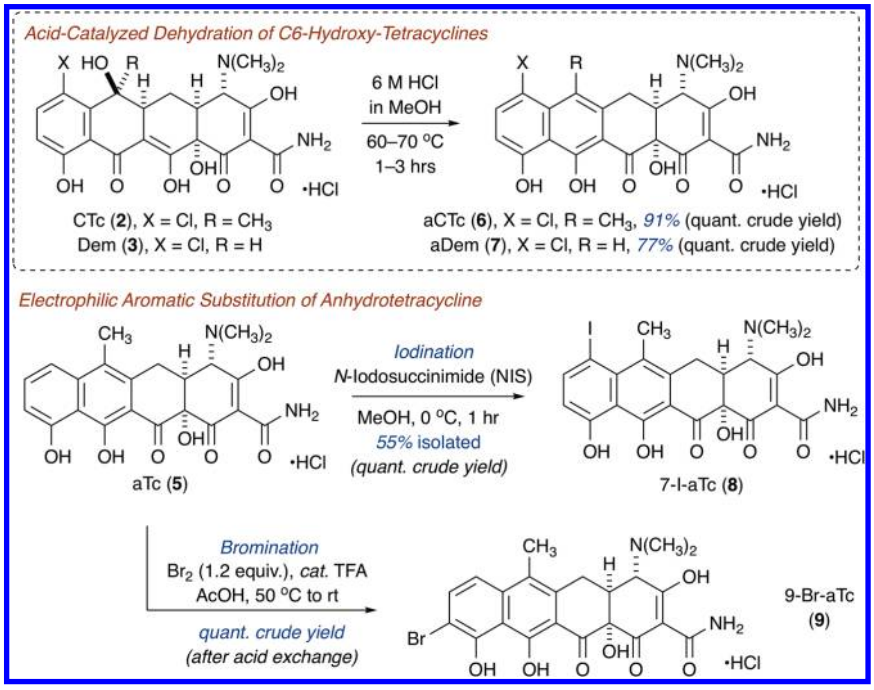

potency fluctuation as a function of enzyme and inhibitor-substrate pairing.

aTC Inhibitory Activity Varies as a Function of Enzyme and Antibiotic Pair. To evaluate the hypothesis that inhibitor potency will vary as a function of enzyme and antibiotic pair, we assessed the *in vitro* inhibitory activity of aTC against the tetracycline destructase-mediated degradation of first-generation tetracycline antibiotics, the results of which are displayed in Figure 4A−D. In general, the apparent half-maximal inhibitory concentrations (IC_{50}s) for the aTC inhibition of Tet(50) were higher than those observed for Tet(X) [5- to 10-fold], with the most potent inhibition observed for Tet(X)_3. Surprisingly, the apparent IC_{50}s observed for the aTC inhibition of tetracycline destructase-mediated degradation of tetracyclines varied modestly as a function of inhibitor-substrate pair within the context of a single enzyme (Figure 4D). However, the half-maximal inhibitory concentrations of aTC inhibition of CTc were

DOI: 10.1021/acsinfecdis.8b00349
ACS Infect. Dis. XXXX, XXX, XXX−XXX

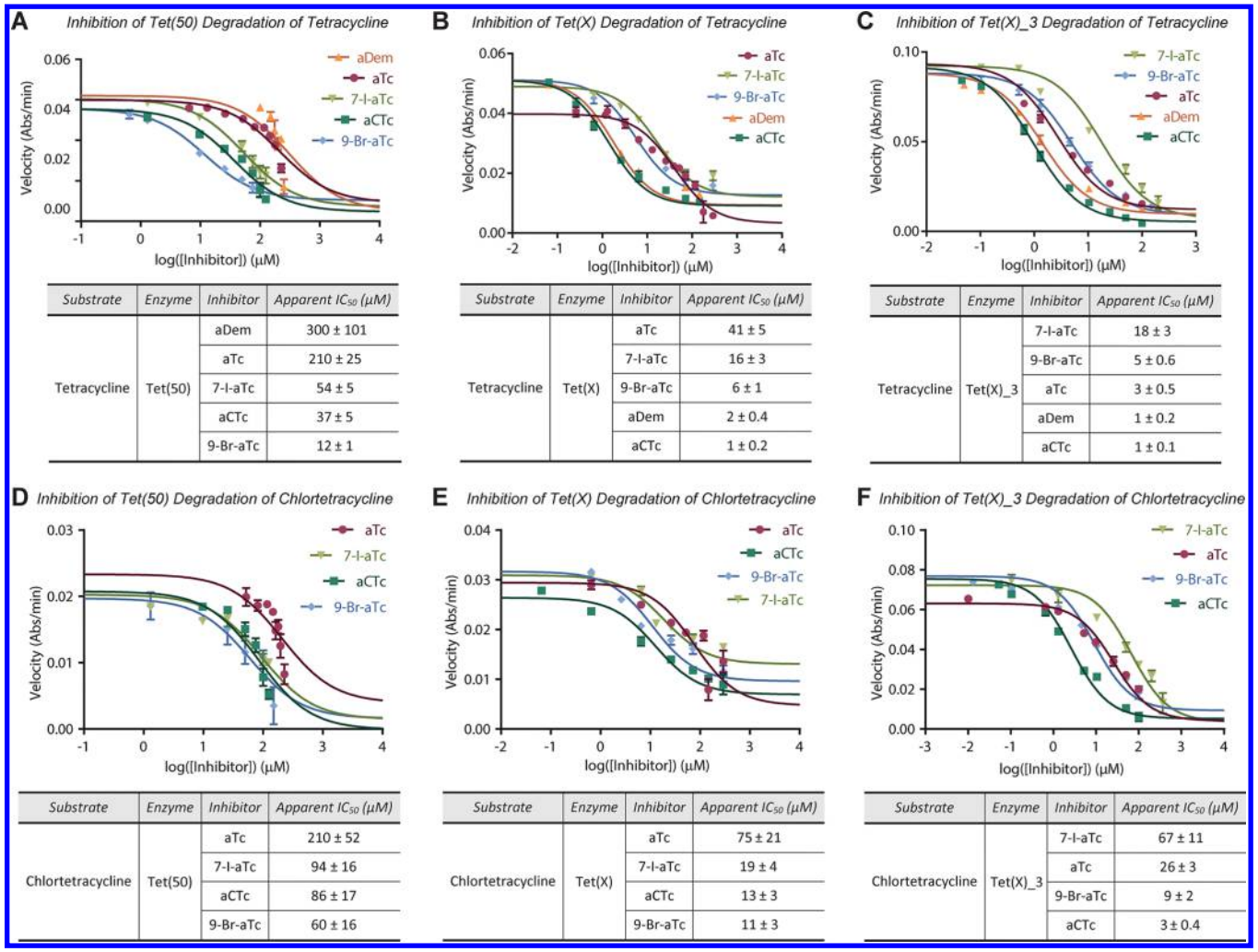

Substrate	Enzyme	Inhibitor	Apparent IC_{50} (μM)
Tetracycline	Tet(50)	aDem	300 ± 101
		aTc	210 ± 25
		7-I-aTc	54 ± 5
		aCTc	37 ± 5
		9-Br-aTc	12 ± 1

Substrate	Enzyme	Inhibitor	Apparent IC_{50} (μM)
Tetracycline	Tet(X)	aTc	41 ± 5
		7-I-aTc	16 ± 3
		9-Br-aTc	6 ± 1
		aDem	2 ± 0.4
		aCTc	1 ± 0.2

Substrate	Enzyme	Inhibitor	Apparent IC_{50} (μM)
Tetracycline	Tet(X)_3	7-I-aTc	18 ± 3
		9-Br-aTc	5 ± 0.6
		aTc	3 ± 0.5
		aDem	1 ± 0.2
		aCTc	1 ± 0.1

Substrate	Enzyme	Inhibitor	Apparent IC_{50} (μM)
Chlortetracycline	Tet(50)	aTc	210 ± 52
		7-I-aTc	94 ± 16
		aCTc	86 ± 17
		9-Br-aTc	60 ± 16

Substrate	Enzyme	Inhibitor	Apparent IC_{50} (μM)
Chlortetracycline	Tet(X)	aTc	75 ± 21
		7-I-aTc	19 ± 4
		aCTc	13 ± 3
		9-Br-aTc	11 ± 3

Substrate	Enzyme	Inhibitor	Apparent IC_{50} (μM)
Chlortetracycline	Tet(X)_3	7-I-aTc	67 ± 11
		aTc	26 ± 3
		9-Br-aTc	9 ± 2
		aCTc	3 ± 0.4

Figure 5. *In vitro* inhibition of tetracycline destructase degradation of first-generation tetracycline antibiotics as observed via optical absorbance kinetic assay. Inhibitory activity of aTC library against (A) Tet(50) degradation of tetracycline, (B) Tet(X) degradation of tetracycline, (C) Tet(X)_3 degradation of tetracycline, (D) Tet(50) degradation of chlortetracycline, (E) Tet(X) degradation of chlortetracycline, and (F) Tet(X)_3 degradation of chlortetracycline. Error bars represent standard deviation for three independent trials. All data points possess error bars, though some are not visible at the plotted scale.

notably higher than those observed for the enzymatic degradation of the other first-generation tetracyclines. In addition, the IC_{50} associated with aTC inhibition of the Tet(X) degradation of oxytetracycline was over an order of magnitude lower than other aTC-tetracycline pairs for the gut-derived enzyme. It is unclear what factors contribute to this effect; however, the combination of lower binding affinity (higher K_m, Figure 3C) and the polyhydroxylated nature of oxytetracycline may allow for more favorable inhibitor competition for the substrate binding pocket—since oxytetracycline may appear more Tet(X) product-like than other tetracycline substrates, *vide infra*.[33]

Analysis of Lineweaver–Burk plots of the aTC inhibition of tetracycline destructase-mediated degradation of tetracycline supports the idea of a mixed competitive/noncompetitive inhibition model (Supporting Information Figure 2). Taken collectively, these results suggest that aTC inhibition involves more than a contest of competitive binding and catalytic efficiency, which is consistent with multicomponent enzyme processes and substrate/inhibitor binding mode flexibility observed for the tetracycline destructase enzymes.[36,38−42] Consequently, because inhibition model ambiguity and binding mode flexibility can complicate broad computational docking to direct the rational design of inhibitors, direct modification of the aTC scaffold may be the most efficient way to aid in the generation of larger inhibitor libraries by determining empirical inhibitor structure−activity relationships (SAR).

Semisynthesis of aTC Analogues. Inspired by the seminal work of Nelson and co-workers, as well as Gmeiner and co-workers, involving semisynthetic strategies to tetracycline and anhydrotetracycline analogues,[43,44] we synthesized four aTC analogues from parent tetracyclines to evaluate the potential for aTC to serve as a privileged scaffold for the development of tetracycline-inactivating enzyme inhibitors (Scheme 1). Acid-catalyzed dehydration of C6-hydroxy-tetracyclines chlortetracycline (CTc, **2**) and demeclocycline (Dem, **3**) provided the corresponding anhydrotetracycline variants, anhydrochlortetracycline (aCTc, **6**) and anhydrodemeclocycline (aDem, **7**) in quantitative crude yields and excellent isolated yields (C18-silica gel, reverse-phase preparative high-performance liquid chromatography (HPLC)). Correspondingly, electrophilic aromatic substitution of anhydrotetracycline (aTC, **5**) with either *N*-iodosuccinimide (NIS)

DOI: 10.1021/acsinfecdis.8b00349
ACS Infect. Dis. XXXX, XXX, XXX−XXX

A

Construct	Substrate	Inhibitor	Substrate MIC (μg/mL)	Inhibitor MIC (μg/mL)	Substrate + [Inhibitor] MIC (μg/mL)	FICI	Fold Change
Tet(50)	Tetracycline	aTC	128	16	32 [4]	0.5	4
	Demeclocycline	aTC	64	8	16 [2]	0.5	4
	Tetracycline	aCTC	128	32	16 [8]	0.38	8
	Chlortetracycline	aCTC	128	32	32 [8]	0.5	4
	Tetracycline	aDem	128	16	32 [8]	0.75	4
	Demeclocycline	aDem	64	16	16 [8]	0.75	4
	Tetracycline	9-Br-aTC	128	16	32 [8]	0.75	4
	Chlortetracycline	9-Br-aTC	128	16	32 [8]	0.75	4
Tet(X)	Tetracycline	aTC	32	16	8 [4]	0.5	4
	Chlortetracycline	aCTC	32	32	8 [4]	0.38	4
	Tetracycline	aDem	32	16	8 [4]	0.5	4
Tet(X)_3	Tetracycline	aTC	512	64	64 [16]	0.38	8
	Chlortetracycline	aTC	256	64	64 [16]	0.5	4
	Chlortetracycline	aCTC	256	128	64 [16]	0.38	4
	Tetracycline	aDem	512	16	64 [4]	0.38	8

B

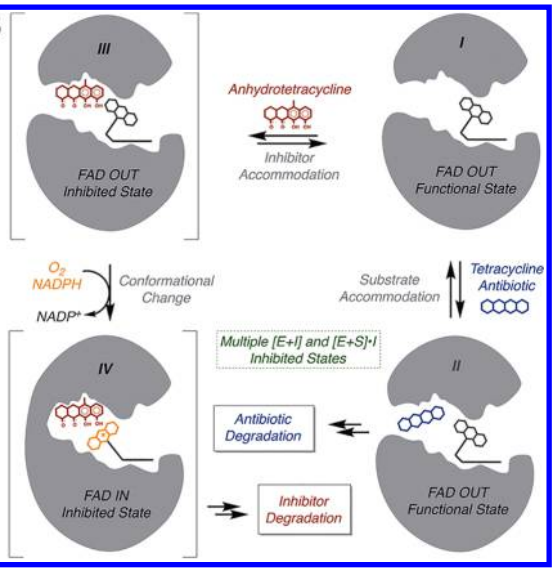

Figure 6. (A) Whole cell inhibition of *E. coli* expressing tetracycline destructase enzymes including calculated FICI and observed fold change enhancements. (B) Working model of the inhibition of tetracycline destructase enzymes by aTC-like small molecules (competitive inhibitor vs sacrificial substrate).

or molecular bromine (in acid) afforded C7-iodoanhydrotetracycline (7-I-aTC, **8**) and C9−Br-anhydrotetracycline (9-Br-aTC, **9**) in excellent crude and isolated yields. These brightly colored solids were storable at low temperatures (−20 °C), away from light, with little decomposition observed over six month periods (by high-performance liquid chromatography−mass spectrometry, LCMS), and stability and longevity improved when the compounds were stored at low temperature under argon atmosphere. However, triturations with methyl-*tert*-butyl ether (MTBE) of analogues with trace impurities, followed by filtration, allowed for reisolation of greater than 90−95% purity material as determined by LCMS and NMR.

Biological Evaluation of aTC Analogue Library. With a scalable synthetic route in hand, we evaluated the ability of the aTC analogues to inhibit tetracycline-destructase enzymes via an *in vitro* optical absorbance kinetic assay and referenced the results to those obtained for known inhibitor, aTC, in parallel scenarios (Figure 5). In general, inhibitor potency varied in an enzyme-dependent manner that was consistent with what was previously observed with aTC, vide supra. Apparent half-maximal inhibitory concentrations (IC_{50}s) were highest for the Tet(50)-mediated degradation of tetracycline and chlortetracycline (Figure 5A,D), followed by Tet(X) (Figure 5B,E) and Tet(X)_3 (Figure 5C,F), respectively. Inhibitor potency decreased (2- to 10-fold) when inhibitors were coadministered with CTc (Figure 5D−F) over tetracycline (Figure 5A−C), and chlorinated aTC analogues aCTc and aDem performed marginally better than aTC when coadministered with tetracycline, suggesting little significant cooperativity/synergism of structurally similar inhibitor-substrate pairs. In general, halogenation of the D-ring improved *in vitro* inhibitory activity, though the enhancement observed for C7-chlorination is more pronounced across all enzyme-antibiotic combinations. Removal of the C6-methyl group was well tolerated for the inhibition of Tet(X) and Tet(X)-homologue, Tet(X)_3; however, aDem performed poorly against tetracycline destructase Tet(50). Proposed reasoning for this phenomenon is discussed later in this report, *vide infra*.

With *in vitro* inhibitor potencies established, we next tested the ability of the aTC analogues to rescue tetracycline activity in whole cell inhibition assays of *E. coli* expressing tetracycline destructase enzymes. By varying concentrations of the tetracycline-inhibitor combinations in a checkboard broth microdilution antibiotic susceptibility assay, we were able to identify the lowest concentration of inhibitor that results in at least a fourfold change in the minimum inhibitory concentration (MIC) of the tetracycline alone; highlights of the checkerboard assay are shown in Figure 6A. Several—not all—tetracycline-inhibitor pairs showed enhanced antibiotic activity, when tetracycline substrates were coadministered with small doses of various inhibitors (four- to eight-fold enhancement over antibiotic alone, Figure 6A). Notably, though aTC was, in general, the least potent of the inhibitor library, it performs well—and on par with the chlorinated analogues, aCTc and aDem—in the whole cell rescue of tetracycline activity. It is important to note that, while some of the aTC analogues possess baseline antibiotic activity alone, antibiotic synergistic killing and destructase inhibition may not be mutually exclusive (Figure 6A), and it is not entirely clear how much of a contribution is made by each mechanism for each combination. The calculated fractional inhibitory concentration index (FICI) is provided for reference.[45] However, the enhancements in MIC observed for several anhydrotetracycline-variant/antibiotic combinations are modest yet promising, and potent *in vitro* destructase inhibition by each of the aTC variants—in combination with these results—suggests that whole cell adjuvant activity could be optimized in the future second generation synthesis of larger aTC-like inhibitor libraries.

While 9-Br-aTC and 7-I-aTC possess potent *in vitro* destructase inhibitory activity, the analogues showed limited activity in whole cell inhibition studies, potentially due to increased instability in solution over time and/or increased reactivity toward enzymatic degradation. In particular, 7-I-aTC showed no inhibitory activity with any enzyme−antibiotic combination against whole cell *E. coli* expressing destructase enzymes. We hypothesized that the instability of 7-I-aTC was

DOI: 10.1021/acsinfecdis.8b00349
ACS Infect. Dis. XXXX, XXX, XXX−XXX

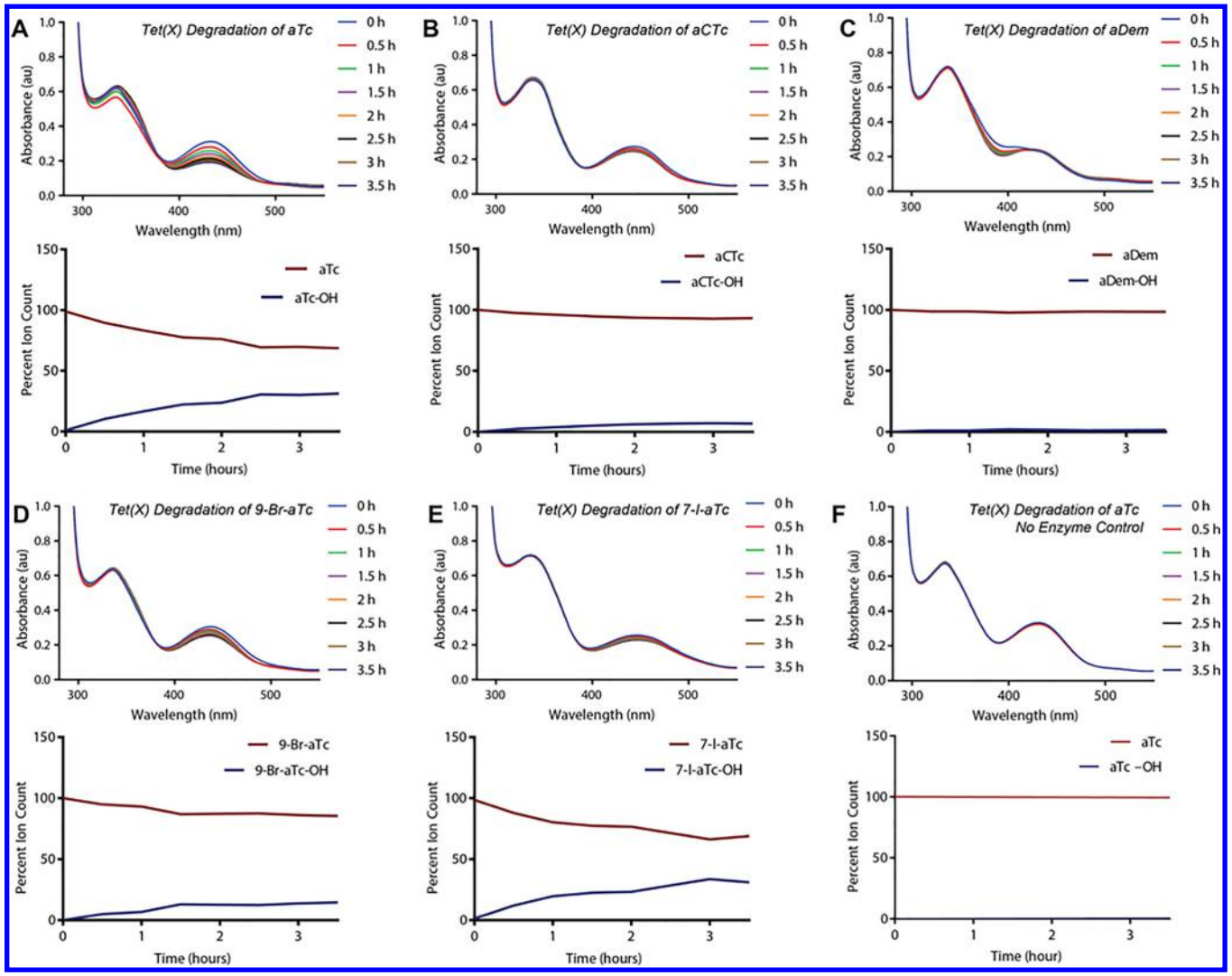

Figure 7. Tet(X)-mediated degradation of aTC and aTC analogues. (A–F) Each panel depicts the degradation of the denoted aTC as observed via optical absorbance spectroscopy and plots of monitored extracted mass counts from LCMS. Each represents a reaction containing purified Tet(X) enzyme (or none, in the case of the control), aTc analogue, and an NADPH regenerating system [including $MgCl_2$]. The plots represent extracted ion counts normalized to an internal standard (Fmoc-alanine) and depicted as a percent of the total ion count [aTC+aTC–OH].

contributing to this phenomenon, as the nonenzymatic degradation of 7-I-aTc in solution was observed by LCMS (overnight) and during extended ^{13}C NMR experiments. Because the *o*/*p*-substitution of phenols with heavy halogens is known to increase the rate of nonenzymatic photooxidation,[46−49] the incorporation of D-ring halogens to future inhibitor libraries may be limited to chlorination and fluorination to preserve inhibitor stability. However, the Br- and I-substituents present in 7-I-aTC and 9-Br-aTC may serve as useful functional handles to access more structurally diverse and stable inhibitor scaffolds. While we propose that disparities in *in vitro* inhibitor potency and whole cell rescue of tetracycline activity are largely due to problems with inhibitor stability, *vide infra*, the potent *in vitro* inhibition of tetracycline destructase enzymes suggests structural modifications that promote inhibitor stability and maintain potency could improve whole cell performance.

Working Inhibition Model. The tetracycline destructase enzymes are class A flavin-monooxygenase (FMO) enzymes that catalyze nicotinamide adenine dinucleotide phosphate (NADPH)- and oxygen-dependent, multicomponent transformations via a series of complex and dynamic conformational changes involving a mobile flavin cofactor.[33,34,38,39] While the precise sequence of events is currently unknown, the proposed degradation process involves substrate recognition and binding to FAD-OUT enzyme conformation **I** (Figure 6B), followed by rapid flavin reduction (FAD to $FADH_2$) by NADPH. Through discrete conformational changes, the reduced flavin cofactor is pushed toward the newly bound substrate and reacts with molecular oxygen to generate the reactive C4a-hydroperoxyflavin in the solvent-protected FAD-IN conformation. The hydroperoxyflavin then reacts with the tetracycline substrate,[33,34,36,39] and another series of conformational changes allows for release of the degradation product and dehydration of the resultant C4a-hydroxyflavin to regenerate FAD-OUT conformer **I**.

Upon the basis of the findings presented herein, in combination with previous studies,[33,34,37] we developed a working model for inhibition of tetracycline destructase enzymes in the context of the proposed degradation process (Figure 6B). In the event that inhibition occurs competitively, inhibitor could bind to substrate unbound enzyme and exclude

DOI: 10.1021/acsinfecdis.8b00349
ACS Infect. Dis. XXXX, XXX, XXX–XXX

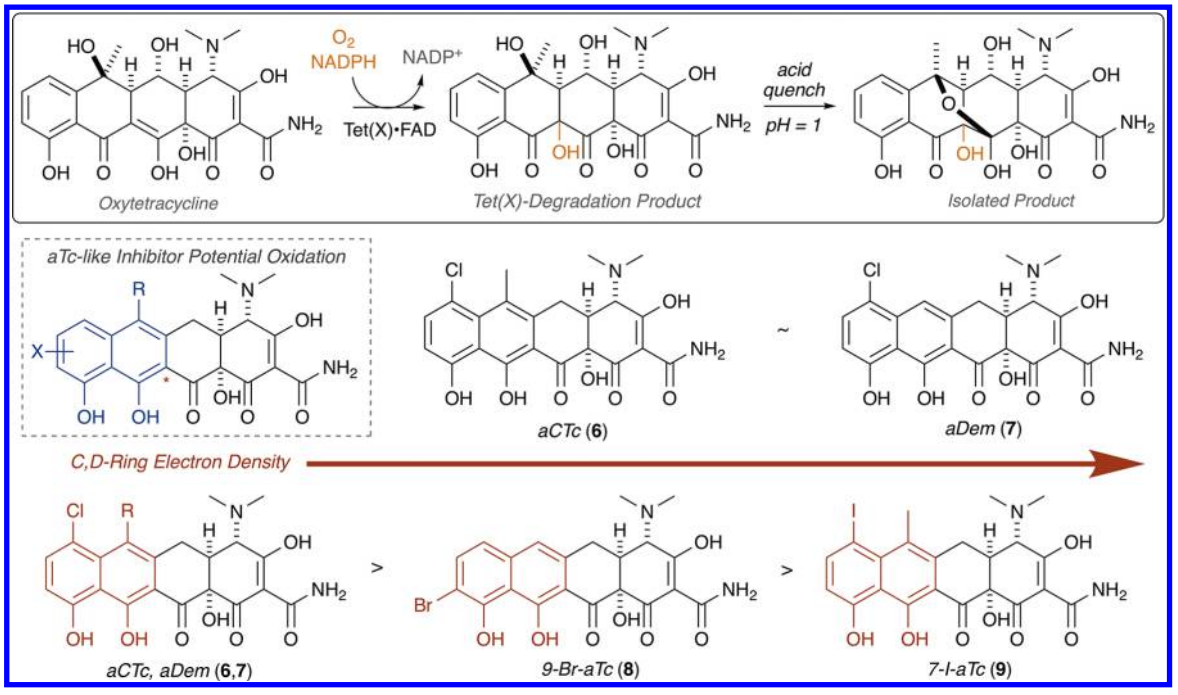

Figure 8. Tet(X)-mediated degradation of oxytetracycline as a model for the degradation of aTC-like sacrificial substrates.

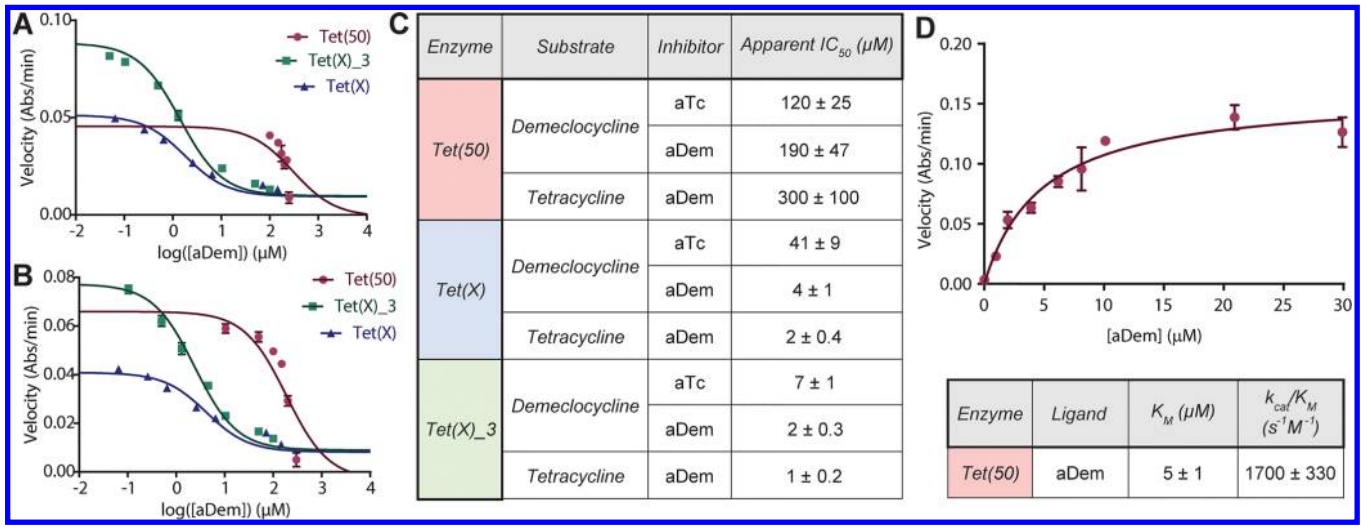

Enzyme	Substrate	Inhibitor	Apparent IC_{50} (μM)
Tet(50)	Demeclocycline	aTc	120 ± 25
		aDem	190 ± 47
	Tetracycline	aDem	300 ± 100
Tet(X)	Demeclocycline	aTc	41 ± 9
		aDem	4 ± 1
	Tetracycline	aDem	2 ± 0.4
Tet(X)_3	Demeclocycline	aTc	7 ± 1
		aDem	2 ± 0.3
	Tetracycline	aDem	1 ± 0.2

Enzyme	Ligand	K_M (μM)	k_{cat}/K_M ($s^{-1}M^{-1}$)
Tet(50)	aDem	5 ± 1	1700 ± 330

Figure 9. aDem inhibition of tetracycline destructase-mediated degradation of first-generation tetracyclines. (A) aDem inhibition of tetracycline destructase degradation of tetracycline. (B) aDem inhibition of tetracycline destructase degradation of demeclocycline. (C) Apparent IC_{50} for the *in vitro* inhibition of tetracycline and demeclocycline degradation by tetracycline destructase enzymes with aTC and aDem. (D) Michaelis–Menten plot of dose-dependent aDem acceleration of Tet(50) consumption of NADPH, apparent K_m, and calculated catalytic efficiency. Error bars represent standard deviation for two to three independent trials. All data points possess error bars, though some are not visible at the plotted scale.

accommodation of substrate into the active site; this inhibited state (**III**) could be a stalled state (nonproductive), or the inhibitor could react with the enzyme as a sacrificial substrate (moving through inhibited state **IV** and multiple successive inhibited states en route to the enzymatic degradation of the inhibitor, Figure 6B). Alternatively, inhibition could occur noncompetitively, where inhibitor binds to substrate-bound enzyme complex (Intermediate **II** or successive substrate-bound functional enzyme states) and restrains the conformational flexibility of the enzyme to impede productive turnover. Because degradation is a complex, multicomponent process involving a number of discrete enzyme conformational changes, none of the multiple inhibited states derived from substrate-bound and substrate-unbound functional enzyme states can implicitly be excluded. Therefore, to assess the potential of the generated aTC analogues to undergo enzymatic degradation as sacrificial substrates, we chose to evaluate the *in vitro* degradation of the inhibitor library by canonical tetracycline-inactivating enzyme, Tet(X), which is known to degrade aTC, albeit slowly.[34]

aTC Analogues as Substrates for Destructase Enzymes. Using Tet(X) as a model system, we assessed the potential for the aTC analogues to serve as sacrificial substrates via an *in vitro*, broad-scan optical absorbance kinetic assay coupled to LCMS, as previously reported for the Tet(X)-mediated degradation of aTC.[34] The results of the Tet(X)-

DOI: 10.1021/acsinfecdis.8b00349
ACS Infect. Dis. XXXX, XXX, XXX−XXX

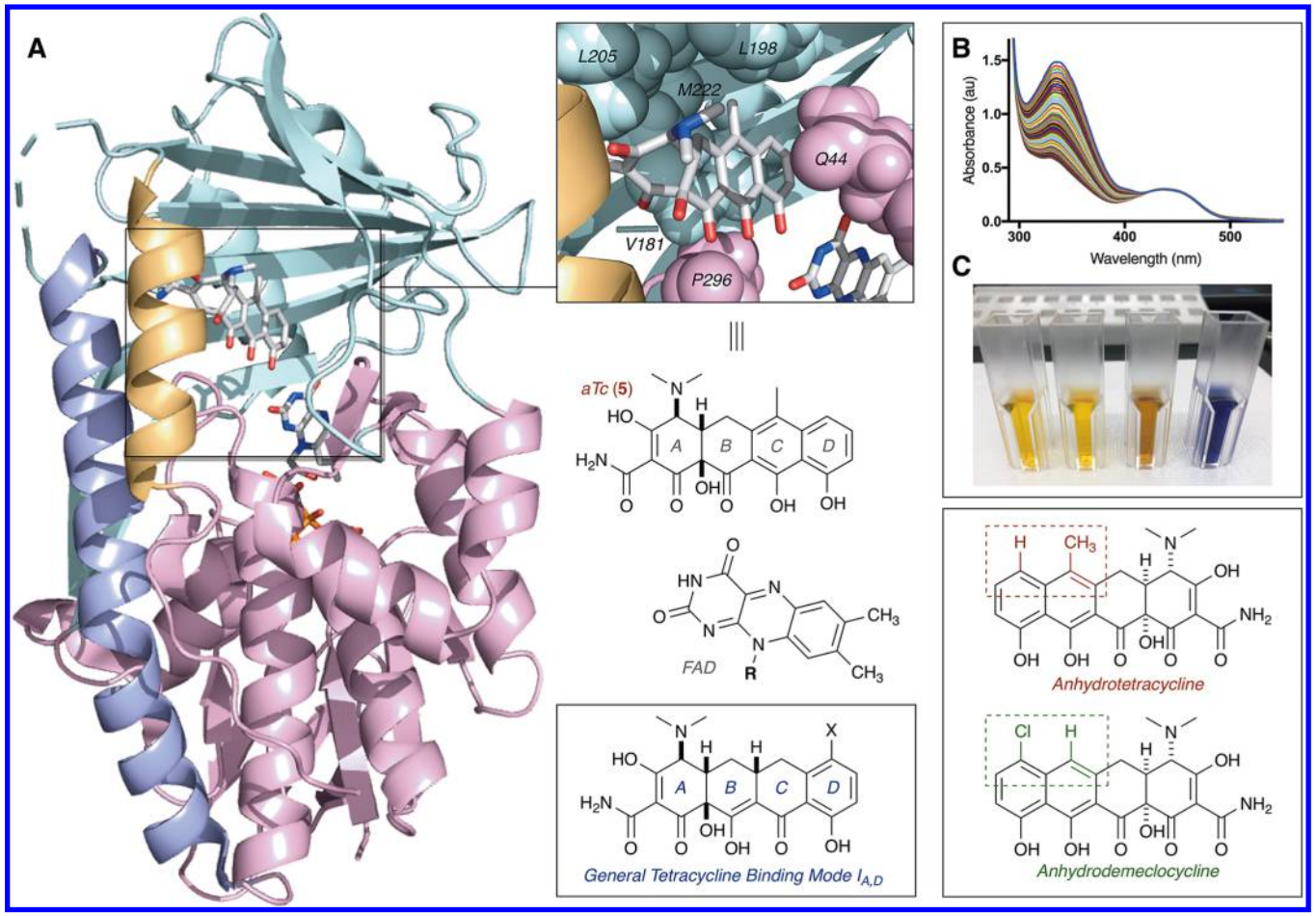

Figure 10. (A) X-ray crystal structure of aTC bound to Tet(50) [PDB ID: 5TUF] and corresponding binding mode identifier; (B) time- and aDem-dependent degradation of NADPH by Tet(50) observed using a broad-scan optical absorbance kinetic assay; (C) hydrogen peroxide colorimetric detection experiments, from left to right: NADPH (no enzyme) control, no enzyme control (NADPH + aDem), Tet(50) + NADPH [no aDem] reaction mixture, and Tet(50) + NADPH + aDem reaction mixture.

mediated aTC analogue degradation assays are summarized below (Figure 7). We confirmed that aTC is a substrate for Tet(X), indicated by the time- and enzyme-dependent decrease in the 440 nm absorption band and aTC extracted mass (LCMS) and used this result as a positive control for the enzymatic degradation of the aTC scaffold. In general, aTC analogue stability increased with D-ring halogenation, and chlorination provided the most "protection" against enzymatic degradation. Moreover, observed stability tracks with degree of electron deficiency and the electron-withdrawing nature of the added substituent (i.e., aCTc is more stable than 9-Br-aTC, which is more stable than 7-I-aTC and aTC, respectively). We hypothesize that this stability is due to decreased nucleophilicity of the C,D-ring aromatic framework, which would be fundamentally important to an enzyme-mediated electrophilic hydroxylation event similar to that determined by Wright and co-workers in 2004 for Tet(X) degradation of oxytetracycline (Figure 8).[33]

Anhydrodemeclocycline, a Special Case. As detailed above, chlorinated aTC analogue anhydrodemeclocycline (aDem, **7**) possesses potent *in vitro* inhibitory activity against the Tet(X)- and Tet(X)_3-mediated degradation of tetracycline antibiotics (apparent IC_{50}s 1−4 μM, Figure 9A−C) and rescues tetracycline activity in whole cell *E. coli* expressing these enzymes (Figure 6A); however, **7** was found to possess poor *in vitro* inhibitory activity against the enzymatic degradation of both tetracycline and demeclocycline by soil-derived tetracycline destructase Tet(50). Moreover, when aDem was exposed to Tet(50) in the presence of NADPH and absence of tetracycline in an optical absorbance kinetic assay, a steady, observable decrease in the absorbance at 400 nm was observed, suggesting that aDem itself was a substrate for Tet(50). To expand upon this observation, we determined kinetic parameters for the aDem dose-dependent response, similar to the Michaelis−Menten parameters previously described (Figure 9D); however, LCMS-coupled experiments for the reaction showed no measurable decrease in aDem extracted mass over time (Supporting Information Figure 3)—suggesting that the decrease in absorbance at 400 nm was the result of rapid, aDem-dependent Tet(50)-mediated consumption of NADPH (broad absorbance band at 340 nm) and not the enzymatic degradation of aDem **7**.

The previously reported X-ray crystal structure of aTC bound to Tet(50) revealed a unique inhibitor binding mode, denoted Mode $I_{A,D}$,[42] resulting from the noncovalent interaction of aTC with residues in both the substrate binding domain and the FAD binding domains of the enzyme (Figure 10A).[37] In particular, the C6-methyl substituent on aTC occupies a small hydrophobic pocket between lysine 198, lysine 205, and methionine 222 of the substrate binding domain. Because this substituent is notably absent in aDem, we hypothesized that binding mode flexibility previously observed

DOI: 10.1021/acsinfecdis.8b00349
ACS Infect. Dis. XXXX, XXX, XXX−XXX

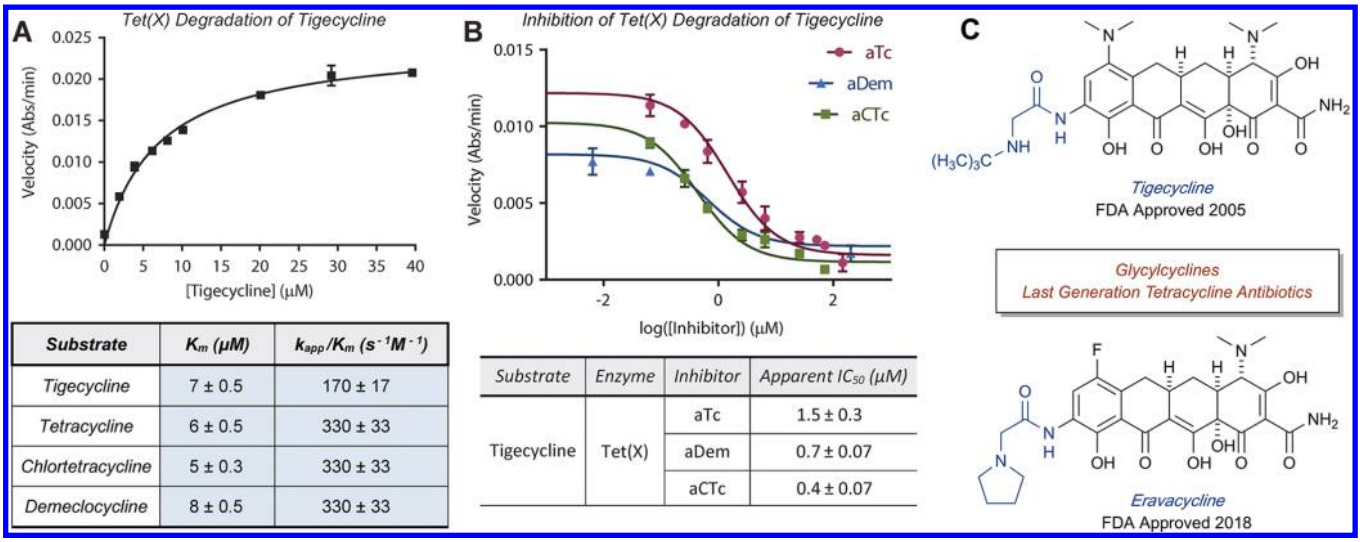

Substrate	K_m (μM)	k_{app}/K_m ($s^{-1}M^{-1}$)
Tigecycline	7 ± 0.5	170 ± 17
Tetracycline	6 ± 0.5	330 ± 33
Chlortetracycline	5 ± 0.3	330 ± 33
Demeclocycline	8 ± 0.5	330 ± 33

Substrate	Enzyme	Inhibitor	Apparent IC_{50} (μM)
Tigecycline	Tet(X)	aTc	1.5 ± 0.3
		aDem	0.7 ± 0.07
		aCTc	0.4 ± 0.07

Figure 11. (A) Michaelis–Menten plot and apparent kinetic parameters (K_m, k_{app}, and catalytic efficiencies) for the Tet(X)-mediated degradation of tigecycline. (B) Inhibitory activity of aTC and chlorinated aTC analogs against Tet(X) degradation of tigecycline. (C) Last-generation tetracycline antibiotics tigecycline and eravacycline. Error bars represent standard deviation for three independent trials. All data points possess error bars, though some are not visible at the plotted scale.

for tetracycline-inactivating enzymes could allow for the accommodation of aDem in a unique, nonreactive binding mode to promote the NADPH-dependent reduction of the mobile flavin element without providing a productive pathway for the degradation of enzyme-bound aDem. Moreover, because the addition of aDem promotes the Tet(50)-mediated consumption of NADPH without resulting in the degradation of aDem itself, we hypothesized that the formation of a reactive hydroperoxyflavin cofactor in the absence of a viable substrate would lead to the release of hydrogen peroxide generated from the nonspecific oxidation of water. The NADPH-dependent formation of hydrogen peroxide from FMOs has been reported previously.[50,51] Thus, we characterized the aDem-promoted, Tet(50)-mediated consumption of NADPH using a broad-scan optical absorbance kinetic assay (Figure 10B) and confirmed the formation of hydrogen peroxide using a colorimetric detection method (Pierce Quantitative Peroxide Assay, ThermoScientific, Figure 10C). The nonspecific formation of hydrogen peroxide was not unique to aDem, as it was also observed in the Tet(50)-mediated degradation of tetracycline (see Supporting Information Figures 4 and 5), confirming that "ligand" binding to the substrate-binding domain promotes the consumption of NADPH and reduction of the mobile flavin cofactor (as is canonical with Class A FMO enzymes).[38] This mode of inhibition is under further investigation in our lab and might prove to be effective against pathogens expressing tetracycline destructases, as a method of inducing oxidative stress by stimulating flavin reduction and release of hydrogen peroxide inside the cell.

Inhibiting Tet(X) Degradation of Third Generation Tetracycline, Tigecycline. The rise of multidrug-resistant superinfections has cultivated a renaissance for tetracycline antibiotics as last-resort treatments.[19] In 2005, the first member of the third-generation tetracyclines tigecycline was Food and Drug Administration (FDA)-approved for the treatment of skin and intra-abdominal infections and pneumonia.[52] Earlier this year, two additional third-generation tetracyclines, eravacycline and omadacycline, were FDA-approved for similar treatment strategies (Figure 11C).[53,54] In this report, we used first-generation tetracyclines as model systems for tetracycline-inactivating enzyme activity; however, with the advent of tigecycline, eravacycline, and omadacycline, the enzymatic degradation of last-generation tetracyclines is fundamentally important to study, since new resistance mechanisms, including antibiotic inactivation, are certain to emerge upon widespread antibiotic deployment. The third-generation tetracyclines were strategically designed to overcome resistance due to efflux and ribosome protection, making antibiotic inactivation a likely candidate for future clinical resistance. Previous reports have identified that Tet(X) can degrade tigecycline and eravacycline, albeit slowly, to achieve resistance to these last-generation tetracyclines.[55−57] Resistance to tigecycline was not observed with the soil-derived tetracycline destructase enzymes, including Tet(50), presumably because the presence of the "Gatekeeper helix" excludes productive accommodation of tetracyclines with bulky D-ring substituents (Figure 2C).[34,37] Building upon previous reports, we confirmed and characterized the Tet(X)-mediated degradation of tigecycline and determined Michaelis–Menten kinetic parameters using an optical absorbance kinetic assay (Figure 11A). After identifying the most promising inhibitor candidates from previously described *in vitro* and whole cell inhibition assays, we evaluated the *in vitro* inhibitory activity of aTC, aCTc, and aDem against the Tet(X)-mediated degradation of tigecycline and found all to be potently inhibitory (apparent IC_{50}s from ∼0.4 to 1.5 μM). Unfortunately, in our hands, whole cell *E. coli* expressing Tet(X) displays minimal resistance to tigecycline (twofold increase over empty vector controls); thus, it was difficult to identify inhibition profiles from variations in the limited resistance response. However, the potent *in vitro* inhibition of aTC, aCTc, and aDem against Tet(X) degradation of tigecycline are promising preliminary results for further development of adjuvant approaches to combat the enzymatic degradation of last-generation tetracyclines. Moreover, because of the functional similarities and phylogenetic clustering of the gut-derived enzymes, we hypothesize that Tet(X)_3 may possess similar abilities to degrade last-generation tetracyclines with velocities more amenable to both *in vitro* and whole cell inhibition assays—though full characterization of Tet(X)_3

DOI: 10.1021/acsinfecdis.8b00349
ACS Infect. Dis. XXXX, XXX, XXX−XXX

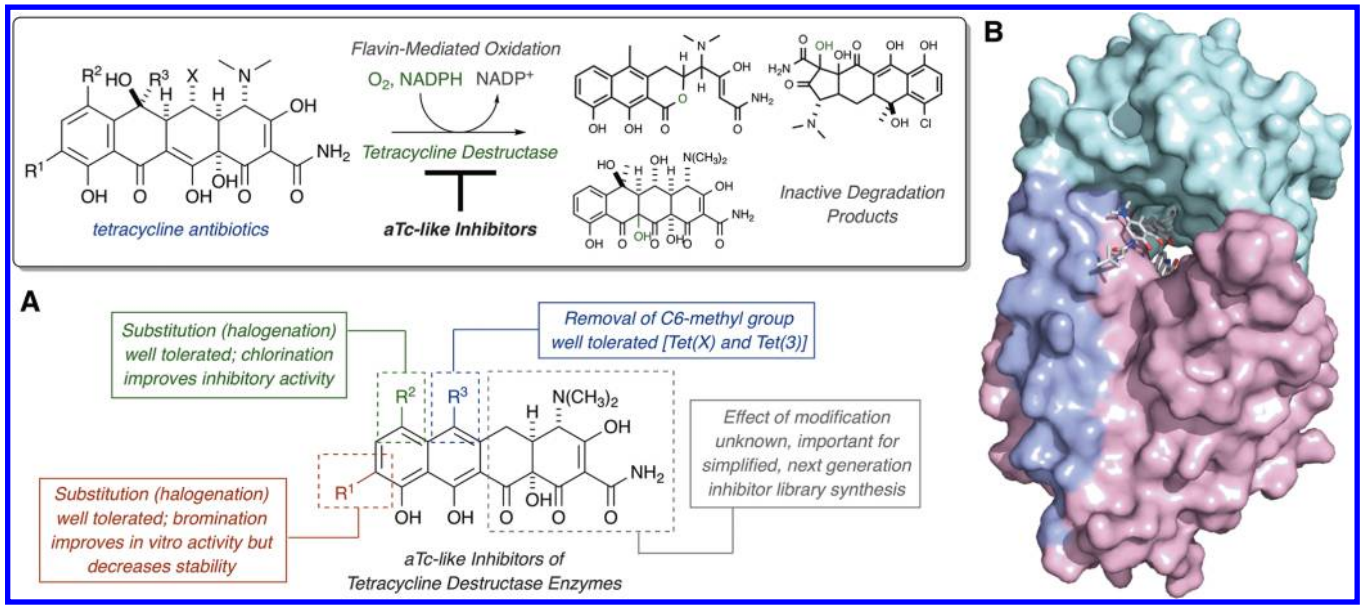

Figure 12. Toward extended library synthesis of aTC-like inhibitors of tetracycline destructase enzymes. (A) An adjuvant approach to combat enzymatic inactivation of tetracycline antibiotics and summary of preliminary structure−activity information. (B) Surface view of X-ray crystal structure of Tet(X) bound to tigecycline (PDB ID 4a6n) highlights importance of open active site to accommodate bulky D-ring substituents, suggesting further use of glycylcycline antibiotics may drive selective pressure of tetracycline destructase-involved resistance mechanisms.

was somewhat beyond the scope of this report. Studies focused on the resistance profile and microbial evolution of tetracycline-inactivating enzyme Tet(X)_3 are currently ongoing in our laboratories and will be reported in due course.

CONCLUSION

In conclusion, the synthesis and biological evaluation of aTC-like small molecule inhibitors of tetracycline-inactivating enzymes are reported (Figure 12A). The four analogues were screened for inhibitory activity against the enzymatic degradation of tetracycline antibiotics by three representative tetracycline destructase enzymes via both *in vitro* and whole cell-based inhibition assays. All synthesized analogues were found to possess *in vitro* inhibitory activity to some degree, and inhibitor potency was found to vary largely as a function of enzyme and moderately as a function of inhibitor−substrate pairing within the context of a single enzyme. The addition of electron-withdrawing groups to the D-ring of aTC was found to improve both the enzymatic and nonenzymatic stability of the aTC analogues, and potent *in vitro* inhibitory activity of this small library shows promise for the rational design of larger tetracycline-inactivating enzyme inhibitor libraries. Notably, aTC and chlorinated analogues aCTc and aDem were found to inhibit the Tet(X)-mediated degradation of last-generation tetracycline, tigecycline. Further development of small molecule inhibitors of glycylcycline-inactivating enzymes like Tet(X), with open active sites that can accommodate large D-ring substituents on tetracycline substrates (Figure 12B),[35] are fundamentally important to establishing viable adjuvant approaches that combat the imminent emergence of this resistance mechanism in multidrug-resistant infections. Efforts aimed at improving inhibitor stability while maintaining potency are currently ongoing in our laboratories and will be reported in due course.

EXPERIMENTAL SECTION

General Methods. Unless stated, all synthetic reactions were performed under inert, argon atmosphere, and all *in vitro* kinetic assays were prepared actively open to air (in nondegassed solvents). All solvents—including deuterated NMR solvents—and reagent chemicals used in preparation or analysis of the aTC analogue library were obtained commercially and used without further purification. IR spectroscopy was performed on a Bruker Alpha FTIR machine with a Pt-ATR diamond, and IR data were analyzed using Bruker OPUS 7.5. Melting points were observed using a Stuart SMP10 digital melting point apparatus. NMR spectra were obtained on a Varian Unity-Plus 300 MHz, Varian Unity-Inova 500 MHz, or Agilent PremiumCompact+ 600 MHz spectrometer. All free induction decay files (FIDs) were processed using Mestrenova version 11.0.4 software. Chemical shifts (δ) are reported in parts per million (ppm) and referenced to residual nondeuterated solvent. Coupling constants (J) are reported in hertz (Hz). High-resolution mass spectrometry data were obtained at the Danforth Plant Science Center (DPSC) in St. Louis, MO, by direct infusion using an Advion Nanomate Triversa robot into a Thermo-Fisher Scientific Q-Exactive mass spectrometer, and mass spectra were recorded in positive ion mode from m/z 150−500 and a resolution setting of 140 000 (at m/z 200). *In vitro* degradation experiments monitored by optical absorbance spectroscopy were performed on an Agilent Cary 50 UV−visible spectrophotometer. *In vitro* degradation experiments monitored by LCMS were performed using an Agilent 6130 single quadrupole instrument with G1313 autosampler, G1315 diode array detector, and 1200 series solvent module and separated using a Phenomenex Gemini C18 column, 50 × 2 mm (5 μm) with guard column cassette and a linear gradient of 0% acetonitrile and 0.1% formic acid to 95% acetonitrile and 0.1% formic acid over 20 min at a flow rate of 0.5 mL/min before analysis by electrospray ionization (ESI+). Whole cell assays were performed using Difco BBL Mueller-Hinton broth

DOI: 10.1021/acsinfecdis.8b00349
ACS Infect. Dis. XXXX, XXX, XXX−XXX

in Costar 96-well plates at 37 °C. End-point growth was assayed at OD_{600} using a Synergy H1 plate reader (BioTek, Inc.).

Cloning, Expression, and Purification of Tetracycline-Destructase Enzymes. All genes corresponding to the tetracycline destructases[34,37] used in this report (for Tet(X)_3, see Supporting Information Table 1) were cloned into pET28b(+) vectors (Novagen) as previously described (*Bam*HI and NdeI restriction sites)[34,37] and transformed into BL21-Star (DE3) competent cells (Life Technologies). Cells were cultured at 37 °C in lysogeny broth (LB) containing kanamycin (0.03 mg/mL); once the uninduced culture reached an OD_{600} of 0.6, the cells were cooled to 0 °C, induced with 1 mM IPTG, and allowed to grow at 15 °C for 12−15 h (harvest OD_{600} varied by tetracycline destructase expressed, but on average, harvest OD_{600} < 4.5 resulted in greater isolated enzyme yield). To harvest, the induced cells were pelleted by centrifugation at 4000 rpm for 15 min (4 °C) and resuspended in cold 40 mL of lysis buffer (50 mM K_2HPO_4, 500 mM NaCl, 20 mM imidazole, 10% glycerol, 5 mM 2-mercaptoethanol, pH 8.0) containing SIGMAFAST protease inhibitor. The cells were transferred to falcon tubes, flash frozen in liquid nitrogen, and stored at −80 °C. To harvest, the cells were thawed and mechanically lysed using an Avestin EmulsiFlex-C5 cell disruptor, and the resultant lysate was centrifuged at 45 000 rpm for 35 min. The supernatant was transferred to a column containing prewashed Ni-NTA resin and incubated for 30−45 min; at which point, the resin was washed with lysis buffer (2 × 40 mL), and the protein was eluted from the resin with fractions of elution buffer (5 × 10 mL, 50 mM K_2HPO_4, 500 mM NaCl, 5 mM β-mercaptoethanol, 300 mM imidazole, 10% glycerol, pH 8.0). The fractions were combined in 10 000 molecular weight cutoff (MWCO) Snakeskin dialysis tubing (ThermoScientific) and soaked in buffer (50 mM K_2HPO_4 pH 8.0, 150 mM NaCl, 1 mM dithiothreitol (DTT)) overnight to minimize imidazole concentration. To isolate the desired protein, the dialyzed solution was concentrated using a 30 000 MWCO Amicon centrifugal filter (Millipore-Sigma), and concentrated protein solution was flash frozen in liquid nitrogen (50 μL portions) and stored at −80 °C.

Kinetic Characterization of Tetracycline Inactivation. Kinetic characterization of tetracycline inactivation was achieved in a manner similar to previously reported procedures.[37] In brief, reaction samples were prepared in [tris(hydroxymethyl)methylamino]propanesulfonic acid (TAPS) buffer (100 mM, pH 8.5) with 504 μM NADPH, 5.04 mM $MgCl_2$, varying concentrations of tetracycline substrate (typically, 0−40 μM), and 0.4 μM enzyme. After the addition of enzyme, the reactions (in duplicate or triplicate) were mixed, manually by pipet, and the reaction was monitored continuously in a single frame by optical absorbance spectroscopy (absorbance at 380 nm, Carey UV−visible spectrophotometer) for 3−4 min. Initial enzyme velocities were determined by linear regression using Agilent Cary WinUV Software over the linear range of the reaction, and the velocities were fitted to the Michaelis−Menten equation[58−60] using GraphPad Prism 6.

Synthesis and Characterization of aTC Analogues 5−8. *(4S,4aS,12aS)-7-Chloro-4-(dimethylamino)-3,10,11,12a-tetrahydroxy-6-methyl-1,12-dioxo-1,4,4a,5,12,12a-hexahydrotetracene-2-carboxamide Hydrochloride (aCTc, **6**).* To a clean, dry round-bottom flask, equipped with stirbar and reflux condenser, was added chlortetracycline hydrochloride (50 mg, 0.10 mmol) and 6 N HCl in methanol (5 mL) under argon atmosphere. The reaction was heated to 60 °C and allowed to stir at 60 °C for 1.5 h (monitored by LCMS). When the reaction was complete, the reaction was concentrated under reduced pressure to provide crude product (50 mg, 0.10 mmol, 100% crude yield) as an orange solid [clean by NMR]. Purification by preparative HPLC (Si−C18 reverse phase column, gradient 0−95% CH_3CN/H_2O with 0.1% formic acid, t_R = 16 min) provided (4*S*,4a*S*,12a*S*)-7-chloro-4-(dimethylamino)-3,10,11,12a-tetrahydroxy-6-methyl-1,12-dioxo-1,4,4a,5,12,12a-hexahydro-tetracene-2-carboxamide, which was reconstituted as the hydrochloride salt to provide the title compound as an orange solid (44 mg, 0.089 mmol, 91% yield). FTIR (neat) 3306, 3042, 1621, 1583, 1565, 1531, 1464, 1375, 1217, 1137, 1058, 820, 560 cm^{-1}; mp 211−212 °C (decomposed); ^1H NMR (500 MHz, deuterated dimethyl sulfoxide (DMSO-d_6)) δ 9.68 (s, 1H), 9.22 (s, 1H), 7.66 (d, J = 8.5 Hz, 1H), 6.88 (d, J = 8.5 Hz, 1H), 4.44 (d, J = 4.0 Hz, 1H), 3.46 (ddt, J = 18.0, 14.2, 4.9 Hz, 2H), 3.15 (dd, J = 16.8, 8.9 Hz, 1H), 2.93 (s, 6H), 2.63 (s, 3H); ^{13}C NMR (126 MHz, DMSO-d_6) δ 199.7, 192.7, 187.4, 172.1, 163.2, 157.6, 136.2, 135.9, 134.1, 121.5, 119.3, 114.6, 111.8, 109.2, 97.6, 76.2, 66.9, 42.9 (2C), 35.8, 29.6, 19.2; high-resolution mass spectrometry (HRMS) (time-of-flight (TOF) MS ES+) calcd for $C_{22}H_{22}ClN_2O_7$ $[M + H]^+$ 461.1116; found 461.1115.

*(4S,4aS,12aS)-7-Chloro-4-(dimethylamino)-3,10,11,12a-tetrahydroxy-1,12-dioxo-1,4,4a,5,12,12a-hexahydrotetracene-2-carboxamide hydrochloride (aDem, **7**).* To a clean, dry round-bottom flask, equipped with stirbar and reflux condenser, was added demeclocycline hydrochloride (50 mg, 0.10 mmol) and 6 N HCl in methanol (5 mL) under argon atmosphere. The reaction was heated to 70 °C and allowed to stir at 60 °C for 3 h (monitored by LCMS). When the reaction was complete, the reaction was concentrated under reduced pressure to provide crude product (54 mg, 0.11 mmol, quant. yield) as a yellow-orange solid (clean by NMR). Purification by preparative HPLC (Si−C18 reverse phase column, gradient 0−95% CH_3CN/H_2O with 0.1% formic acid, t_R = 15 min) to provide (4*S*,4a*S*,12a*S*)-7-chloro-4-(dimethylamino)-3,10,11,12a-tetrahydroxy-1,12-dioxo-1,4,4a,5,12,12a-hexahydrotetracene-2-carboxamide, which was reconstituted as the hydrochloride salt to provide the title compound as a light orange solid (37 mg, 0.077 mmol, 77% yield). FTIR (neat) 3301, 3076, 1619, 1567, 1533, 1444, 1375, 1353, 1202, 1188, 1071, 993, 820, 685 cm^{-1}; mp 213−214 °C (decomposed); ^1H NMR (500 MHz, DMSO-d_6) δ 9.69 (s, 1H), 9.29 (s, 1H), 7.68 (d, J = 8.4 Hz, 1H), 7.39 (s, 1H), 6.92 (d, J = 8.5 Hz, 1H), 4.46 (d, J = 6.5 Hz, 1H), 3.58 (dd, J = 17.3, 4.0 Hz, 1H), 3.53−3.39 (m, 2H), 2.89 (s, 6H); ^{13}C NMR (126 MHz, DMSO-d_6) δ 198.3, 193.1, 187.2, 172.2, 165.2, 157.2, 135.9, 135.2, 132.7, 119.2, 113.9, 113.5, 111.3, 109.7, 97.5, 76.8, 66.4, 42.3, 41.6, 37.2, 29.5; HRMS (TOF MS ES+) calcd for $C_{21}H_{20}ClN_2O_7$ $[M + H]^+$ 447.0959; found 447.0958.

*(4S,4aS,12aS)-4-(Dimethylamino)-3,10,11,12a-tetrahydroxy-7-iodo-6-methyl-1,12-dioxo-1,4,4a,5,12,12a-hexahydrotetracene-2-carboxamide hydrochloride (7-I-aTC, **8**).* **Procedure A**—To a clean, dry round-bottom flask, equipped with stirbar, was added anhydrotetracycline hydrochloride (100 mg, 0.216 mmol) and methanol (2.2 mL) under argon atmosphere. The flask was cooled to −10 °C, and *N*-iodosuccinimide (58.3 mg, 0.259 mmol) was added in one portion. The reaction was allowed to warm to room 0 °C over

DOI: 10.1021/acsinfecdis.8b00349
ACS Infect. Dis. XXXX, XXX, XXX−XXX

2 h, then stirred at 0 °C for 1 h (monitored by LCMS). When the reaction was complete, the reaction was diluted with methanol (to 10 mL total volume) and immediately purified by preparative HPLC (Si−C18 reverse phase column, gradient 0−95% CH_3CN/H_2O with 0.1% formic acid, t_R = 16 min) to provide (4*S*,4a*S*,12a*S*)-4-(dimethylamino)-3,10,11,12a-tetrahydroxy-7-iodo-6-methyl-1,12-dioxo-1,4,4a,5,12,12a-hexahydrotetracene-2-carboxamide, which was reconstituted as the hydrochloride salt to provide the title compound as an orange solid (70.0 mg, 0.119 mmol, 55% yield).

Procedure B−To a clean, dry round-bottom flask, equipped with stirbar, was added anhydrotetracycline hydrochloride (250 mg, 0.540 mmol) and methanol (25 mL) under argon atmosphere. The flask was cooled to 0 °C, and solid *N*-iodosuccinimide (0.134 g) was added, in one portion. The reaction stirred at 0 °C for 1 h (monitored by LCMS), and the reaction was concentrated under reduced pressure (no heating) to yield a crude brown solid. The solid was triturated with *tert*-butylmethyl ether (TBME) for 30 min protected from light; filtration provided the title product (0.3178 g, 0.540 mmol, quantitative crude yield) as a green-brown solid. FTIR (neat) 3307, 3078, 1660, 1615, 1556, 1396, 1377, 1321, 1228, 1131, 1075, 1058, 810, 702, 618 cm^{-1}; mp 188−189 °C; ^1H NMR (500 MHz, DMSO-d_6) δ 9.62 (s, 1H), 9.23 (s, 1H), 8.01 (d, J = 8.9 Hz, 1H), 7.31 (d, J = 8.9 Hz, 1H), 4.38 (s, 1H), 3.57−3.36 (m, 3H), 3.16 (s, 1H), 2.89 (s, 6H), 2.56 (s, 1H), 2.40 (s, 3H); ^{13}C NMR (126 MHz, DMSO-d_6) δ 199.5, 192.9, 187.2, 179.3, 163.7, 156.2, 141.4, 138.5, 130.5, 121.6, 117.2, 112.2, 108.7, 97.4, 79.6, 76.3, 67.0, 42.1 (2C), 35.8, 29.5, 14.1; HRMS (TOF MS ES+) calcd for $C_{22}H_{22}IN_2O_7$ $[M + H]^+$ 553.0472; found 553.0469.

*(4S,4aS,12aS)-9-Bromo-4-(dimethylamino)-3,10,11,12a-tetrahydroxy-6-methyl-1,12-dioxo-1,4,4a,5,12,12a-hexahydrotetracene-2-carboxamide hydrochloride (9-Br-aTC, **9**).* To a clean, dry round-bottom flask, equipped with a stirbar and argon inlet, was added liquid bromine (13 μL, 0.2592 mmol, 1.2 equiv), acetic acid (10 mL), and trifluoroacetic acid (2 μL, 0.0216 mmol, 0.1 equiv). The mixture was heated to 50 °C (over 20 min), at which point anhydrotetracycline hydrochloride (100 mg, 0.216 mmol) was added in one portion. The reaction mixture stirred at 50 °C for 30 min; then, the reaction was cooled to room temperature and stirred at room temperature for 4 h (monitored by LCMS). After the reaction was complete, the crude mixture was concentrated under reduced pressure to provide the crude product, which was reconstituted with aqueous HCl to provide the title compound (0.1165 g, 0.215 mmol, quantitative crude yield) as an orange solid HCl salt. FTIR (neat) 3295, 3078, 1618, 1553, 1393, 1373, 1317, 1224, 1124, 1058, 699, 620 cm^{-1}; mp 203−204 °C (decomposed); ^1H NMR (500 MHz, DMSO-d_6) δ 9.64 (s, 1H), 9.22 (s, 1H), 7.84 (d, J = 9.0 Hz, 1H), 7.42 (d, J = 9.1 Hz, 1H), 4.44 (d, J = 4.0 Hz, 1H), 3.56 (dd, J = 17.7, 4.9 Hz, 1H), 3.46 (dd, J = 9.9, 4.7 Hz, 1H), 3.07 (d, J = 14.5 Hz, 1H), 2.91 (s, 6H), 2.39 (s, 3H); ^{13}C NMR (126 MHz, DMSO-d_6) δ 200.6, 192.7, 187.0, 172.1, 161.8, 153.4, 137.7, 135.8, 131.6, 122.3, 116.7, 112.6, 109.3, 104.5, 97.3, 76.4, 67.0, 42.1 (2C), 35.3, 21.1, 14.0; HRMS (TOF MS ES+) calcd for $C_{22}H_{22}BrN_2O_7$ $[M + H]^+$ 505.0610; found 505.0610.

In Vitro Characterization of aTC and aTC Analogue Inhibition. Half-maximal inhibitory concentrations (IC_{50}) for the aTC and aTC analogue inhibition of Tet(50), Tet(X), and Tet(X)_3 were determined from the nonlinear regression analysis of initial velocities of tetracycline degradation in the presence of varying concentrations of chosen inhibitor. Reaction samples were prepared in 100 mM TAPS buffer (pH 8.5) with 504 μM NADPH, 5.04 mM $MgCl_2$, 25.3 μM tetracycline substrate, varying concentrations of inhibitor (μM), and 0.4 μM enzyme. After the addition of enzyme, the reactions (in triplicate) were mixed manually by pipet, and the reaction was monitored, continuously in a single frame, by optical absorbance spectroscopy (absorbance at 380 or 400 nm, Carey UV−visible spectrophotometer) for 4 min. Initial enzyme velocities were determined by linear regression using Agilent Cary WinUV Software over the linear range of the reaction. The velocities were plotted against the logarithm of inhibitor concentration, and IC_{50} values were determined using nonlinear regression analysis in Graphpad Prism 6. Plus/minus error values were determined using linear regression analysis of initial velocities versus concentrations of inhibitor in Graphpad Prism 6. Each set of experiments was accompanied by a variety of controls, including a no-enzyme control (NADPH + Tet + inhibitor)—which was used to simulate full enzyme inhibition and assigned to inhibitor concentration of 1×10^{15}, and a no-inhibitor control (NADPH + Tet + enzyme)—which was assigned an inhibitor concentration of 1×10^{-15}. A no-substrate control (NADPH + inhibitor + Tet) was also performed to identify competitive background signals from the enzymatic degradation of the inhibitor itself. For all inhibitor−enzyme combinations (except for Tet(50)−aDem), the initial velocities of the no-substrate controls were negligible.

Checkerboard Whole Cell Inhibition Assay. Substrates and inhibitors were dissolved DMSO before being diluted to working concentrations in cation-adjusted Mueller−Hinton broth supplemented with 50 μg/mL kanamycin. A twofold dilution series of each drug was made independently across 8 rows of a 96-well master plate before 100 μL of each drug dilution series was combined into a 96-well culture plate (Costar), with rows included for no-drug and no-inocula controls. The plates were inoculated with ∼1 μL of tetracycline destructase expressing *E. coli* MegaX (Invitrogen) diluted to OD_{600} 0.1 using a sterile 96-pin replicator (Scinomix). Plates were sealed with Breathe-Easy membranes (Sigma-Aldrich) and incubated at 37 °C with shaking at 220 rpm. End-point growth was assayed at OD_{600} at 20 and 36 h of growth using a Synergy H1 plate reader (BioTek, Inc.). Three independent replicates were performed for each strain/drug combination. Highlighted MIC data were refined from a complete raw data set to identify mixtures resulting in the largest MIC fold change (at least fourfold) with the least amount of inhibitor (fold change/inhibitor dose; see Figure 6A and Supporting Information Tables 2a−c). Synergy of inhibitor and tetracycline combinations was determined using the fractional inhibitory concentration index (FICI) method[45]

$$\mathrm{FICI} = \frac{\mathrm{MICA}_{\mathrm{combo}}}{\mathrm{MICA}_{\mathrm{alone}}} + \frac{\mathrm{MICB}_{\mathrm{combo}}}{\mathrm{MICB}_{\mathrm{alone}}} \quad (1)$$

where FICI > 1 indicates antagonism, FICI = 1 indicates additivity, and FICI < 1 indicates synergy.

Kinetic Characterization of aTC and aTC Analogue Degradation by Tet(X). The kinetic characterization of the degradation of aTC and aTC analogues by Tet(X) was monitored by optical absorbance spectroscopy (Carey UV−visible spectrophotometer) coupled to LCMS detection (Agilent 6130 single quadrupole instrument with G1313 autosampler, G1315 diode array detector, and 1200 series

DOI: 10.1021/acsinfecdis.8b00349
ACS Infect. Dis. XXXX, XXX, XXX−XXX

solvent module and separated using a Phenomenex Gemini C18 column, 50 × 2 mm (5 μm) with guard column cassette and a linear gradient of 0% acetonitrile and 0.1% formic acid to 95% acetonitrile and 0.1% formic acid over 20 min at a flow rate of 0.5 mL/min before analysis by electrospray ionization (ESI+)). Reactions (in duplicate) were prepared in 100 mM TAPS buffer (pH 8.5) with an NADPH regenerating system (40 mM glucose-6-phosphate, 4 mM $NADP^+$, 1 mM $MgCl_2$, 4 U/mL glucose-6-phosphate dehydrogenase), 28.0 μM substrate (aTC or corresponding analogue), and 0.24 μM enzyme. Reaction progress was monitored by optical absorbance spectroscopy (280−550 nm, 1 nm and 30 min intervals) over 3.5 h, where 150 μL of reaction sample was removed at 30 min intervals and quenched with 600 μL volumes of quench solution (1:1 acetonitrile/0.25 M aqueous HCl). The quenched samples were centrifuged (5000 rpm, room temperature) for 5 min, and 600 μL of supernatant was transferred to an LCMS-compatible vial containing Fmoc-alanine internal standard (2.21 μM final concentration) and analyzed by LCMS (reverse-phase HPLC, C18-silica, gradient 0−95% CH_3CN/H_2O, 0.5 mL/min flow rate). Substrate masses $[M + H]^+$ and hydroxylated product masses $[M-OH+H]^+$ were extracted from the crude mass chromatogram and normalized to the internal standard $[M + H]^+$ counts. No enzyme controls were performed for each aTC analogue screened and showed no significant nonenzymatic degradation over the course of the observable reaction. Degradation of 7-I-aTC and 9-Br-aTC at extended solution times (overnight) showed a decrease in LCMS extracted ion counts for both analogues, suggesting some nonenzymatic degradation over longer reaction times.

Qualitative Detection of aDem-promoted Hydrogen Peroxide Formation by Tet(50). Qualitative colorimetric detection of aDem-promoted hydrogen peroxide formation by Tet(50) was performed using an aqueous Pierce Quantitative Peroxide Assay kit (ThermoScientific). Reaction samples were prepared in 100 mM TAPS buffer (pH 8.5) with 252 μM NADPH, 2.52 mM $MgCl_2$, 25 μM substrate (either aDem or Tet), and 0.4 μM enzyme. After the addition of enzyme, the reaction was mixed manually by pipet, and the reaction was monitored by optical absorbance spectroscopy (280−550 nm, 1 nm and 0.1 min scan intervals) over 8 min. At 8 min, 100 μL of reaction solution was added to a detection Eppendorf containing 1000 μL of working reagent (prepared according to specifications for Pierce Quantitative Peroxide Assay kit). The detection Eppendorf was incubated for 20 min at room temperature to result in the observed color changes reported in the main text (see Figure 10C and Supporting Information Figure 5).

■ ASSOCIATED CONTENT

Supporting Information

The Supporting Information is available free of charge on the ACS Publications website at DOI: 10.1021/acsinfecdis.8b00349.

Relevant strains, sequences, plasmids, and primers, SDS-page gel images of purified enzyme, Lineweaver−Burk plots, methods for the aTC inhibition of the tetracycline destructase-mediated degradation of tetracycline, expanded data tables for whole cell inhibition assays of *E. coli* expressing tetracycline destructase enzymes, *in vitro* characterization of the aDem- and Tet-promoted consumption of NADPH by Tet(50), images for the qualitative colorimetric detection of Tet- and aDem-promoted hydrogen peroxide formation by Tet(50), and NMR spectra of synthesized compounds **6**−**9** (PDF)

■ AUTHOR INFORMATION

Corresponding Authors

*E-mail: wencewicz@wustl.edu. (T.A.W.)
*E-mail: dantas@wustl.edu. (G.D.)
*E-mail: niraj.tolia@nih.gov. (N.H.T.)

ORCID

Jana L. Markley: 0000-0001-6855-7161
Andrew J. Gasparrini: 0000-0002-4551-4633
Hirdesh Kumar: 0000-0002-8488-3001
Niraj H. Tolia: 0000-0002-2689-1337
Gautam Dantas: 0000-0003-0455-8370
Timothy A. Wencewicz: 0000-0002-5839-6672

Author Contributions

[∇]These authors jointly supervised this work. The manuscript was written through the collaborative contributions of all authors. All authors have given approval to the final version of the manuscript.

Funding

This research is supported by the National Institute of Allergy and Infectious Diseases (NIAID-NIH R01-123394). N.T. is supported by the Intramural Research Program of the National Institute of Allergy and Infectious Diseases, National Institutes of Health. J.L.M. is supported by the W. M. Keck Program in Molecular Medicine.

Notes

The authors declare no competing financial interest.

■ ACKNOWLEDGMENTS

The authors would like to thank Washington Univ. in St. Louis (WUSTL), Washington Univ. School of Medicine, and the National Institutes of Health for their support of this research and our programs. In particular, N.T. would like to thank the Intramural Research Program of the National Institute of Allergy and Infectious Diseases, National Institutes of Health, for the support of his program. We would also like to acknowledge J. Kao and M. Singh (WUSTL, Dept. of Chemistry) for their assistance with NMR experiments and B. Evans (Danforth Plant Science Center, St. Louis, MO) and his team for their assistance in acquiring high-resolution mass spectra for all synthesized compounds. In addition, J.L.M. would like to acknowledge the WM Keck Postdoctoral Program in Molecular Medicine for funding support of her postdoctoral fellowship.

■ ABBREVIATIONS

Tet, tetracycline; CTc, chlortetracycline; Dem, demeclocycline; Oxy, oxytetracycline; aTC, anhydrotetracycline; aCTc, anhydrochlortetracycline; aDem, anhydrodemeclocycline; 7-I-aTC, 7-iodoanhydrotetracycline; 9-Br-aTC, 9-bromoanhydrotetracycline; FMO, flavin-dependent monooxygenases; NADPH, nicotinamide adenine dinucleotide phosphate reduced form; FAD, flavin adenine dinucleotide; HPLC, high-performance liquid chromatography; LCMS, liquid chromatography−mass spectrometry; NMR, nuclear magnetic resonance spectroscopy; IR, infrared spectroscopy; mp, melting point

DOI: 10.1021/acsinfecdis.8b00349
ACS Infect. Dis. XXXX, XXX, XXX−XXX

REFERENCES

(1) Paine, T. F., Collins, H. S., and Finland, M. (1948) Bacteriologic Studies on Aureomycin. *J. Bacteriol. 56*, 489−497 PMCID: PMC518610 .

(2) The history of tetracycline antibiotics in the treatment of human and livestock has been extensively reviewed. For some recent reviews, see: Nelson, M. L., and Levy, S. B. (2011) The History of the Tetracyclines. *Ann. N. Y. Acad. Sci. 1241*, 17−32.

(3) Bahrami, F., Morris, D. L., and Pourgholami, M. H. (2012) Tetracyclines: Drugs with Huge Therapeutic Potential. *Mini-Rev. Med. Chem. 12*, 44−52.

(4) Griffin, M. O., Fricovsky, E., Ceballos, G., and Villarreal, F. (2010) Tetracyclines: a Pleitropic Family of Compounds with Promising Therapeutic Properties. Review of the Literature. *Am. J. Physiol. Cell Physiol. 299*, C539−C548.

(5) Grossman, T. H. (2016) Tetracycline Antibiotics and Resistance. *Cold Spring Harbor Perspect. Med. 6*, a025387.

(6) Nguyen, F., Starosta, A. L., Arenz, S., Sohmen, D., Donhofer, A., and Wilson, D. N. (2014) Tetracycline Antibiotics and Resistance Mechanisms. *Biol. Chem. 395*, 559−575.

(7) Daghrir, R., and Drogui, P. (2013) Tetracycline Antibiotics in the Environment: a Review. *Environ. Chem. Lett. 11*, 209−227.

(8) Zakeri, B., and Wright, G. D. (2008) Chemical Biology of Tetracycline Antibiotics. *Biochem. Cell Biol. 86*, 124−136.

(9) Thaker, M., Spanogiannopoulos, P., and Wright, G. D. (2010) The Tetracycline Resistome. *Cell. Mol. Life Sci. 67*, 419−431.

(10) Liu, F., and Myers, A. G. (2016) Development of a Platform for the Discovery and Practical Synthesis of New Tetracycline Antibiotics. *Curr. Opin. Chem. Biol. 32*, 48−57.

(11) Burke, M. D. (2009) Flexible Tetracycline Synthesis Yields Promising Antibiotics. *Nat. Chem. Biol. 5*, 77−79.

(12) Chopra, I., and Roberts, M. (2001) Tetracycline Antibiotics: Mode of Action, Applications, Molecular Biology, and Epidemiology of Bacterial Resistance. *Microbiol. Mol. Biol. Rev. 65*, 232−260.

(13) Kasbekar, N. (2006) Tigecycline: A New Glycylcycline Antimicrobial Agent. *Am. J. Health-Syst. Pharm. 63*, 1235−1243.

(14) Rose, W. E., and Rybak, M. J. (2006) Tigecycline: First of a New Class of Antimicrobial Agents. *Pharmacotherapy 26*, 1099−1110.

(15) Sutcliffe, J. A., O'Brien, W., Fyfe, C., and Grossman, T. H. (2013) Antibacterial Activity of Eravacycline (TP-434), a Novel Fluorocycline, Against Hospital and Community Pathogens. *Antimicrob. Agents Chemother. 57*, 5548−5558.

(16) Ronn, M., Zhu, Z., Hogan, P. C., Zhang, W.-Y., Niu, J., Katz, C. E., Dunwoody, N., Gilicky, O., Deng, Y., Hunt, D. K., He, M., Chen, C.-L., Sun, C., Clark, R. B., and Xiao, X.-Y. (2013) Process R&D of Eravacycline: the First Fully Synthetic Fluorocycline in Clinical Development. *Org. Process Res. Dev. 17*, 838−845.

(17) Macone, A. B., Caruso, B. K., Leahy, R. G., Donatelli, J., Weir, S., Draper, M. P., Tanaka, S. K., and Levy, S. B. (2014) In Vitro and In Vivo Antibacterial Activities of Omadacycline, a Novel Aminomethylcycline. *Antimicrob. Agents Chemother. 58*, 1127−1135.

(18) Zhanel, G. G., Homenuik, K., Nichol, K., Noreddin, A., Vercaigne, L., Embil, J., Gin, A., Karlowsky, J. A., and Hoban, D. J. (2004) The Glycylcyclines: a Comparative Review with the Tetracyclines. *Drugs 64*, 63−88.

(19) Ruhe, J. J., Monson, T., Bradsher, R. W., and Menon, A. (2005) Use of Long-Acting Tetracyclines for Methicillin-Resistant Staphylococcus aureus Infections: Case Series and Review of the Literature. *Clin. Infect. Dis. 40*, 1429−34.

(20) Huttner, B., Jones, M., Rubin, M. A., Neuhauser, M. M., Gundlapalli, A., and Samore, M. (2012) Drugs of Last Resort? The Use of Polymyxins and Tigecycline at US Veterans Affairs Medical Centers, 2005−2010. *PLoS One 7*, No. e36649.

(21) Theuretzbacher, U., Van Bambeke, F., Canton, R., Giske, C. G., Mouton, J. W., Nation, R. L., Paul, M., Turnidge, J. D., and Kahlmeter, G. (2015) Reviving Old Antibiotics. *J. Antimicrob. Chemother. 70*, 2177−2181.

(22) Connell, S. R., Tracz, D. M., Nierhaus, K. H., and Taylor, D. E. (2003) Ribosomal Protection Proteins and Their Mechanism of Tetracycline Resistance. *Antimicrob. Agents Chemother. 47*, 3675−3681.

(23) Piddock, L. J. V. (2006) Clinically Relevant Chromosomally Encoded Multidrug Resistance Efflux Pumps in Bacteria. *Clin. Microbiol. Rev. 19*, 382−402.

(24) Davies, J. (1994) Inactivation of Antibiotics and the Dissemination of Resistance Genes. *Science 264*, 375−382.

(25) Wright, G. D. (2005) Bacterial Resistance to Antibiotics: Enzymatic Degradation and Modification. *Adv. Drug Delivery Rev. 57*, 1451−1470.

(26) Bush, K., and Jacoby, G. A. (2010) Updated Functional Classification of beta-Lactamases. *Antimicrob. Agents Chemother. 54*, 969−976.

(27) Brandt, C., Braun, S. D., Stein, C., Slickers, P., Ehricht, R., Pletz, M. W., and Makarewicz, O. (2017) In Silico Serine beta-Lactamases Analysis Reveals a Huge Potential Resistome in Environmental and Pathogenic Species. *Sci. Rep. 7*, 43232.

(28) Kong, K.-F., Schneper, L., and Mathee, K. (2010) Beta-Lactam Antibiotics: From Antibiosis to Resistance and Bacteriology. *APMIS 118*, 1−36.

(29) Perez-Llarena, F. J., and Bou, G. (2009) Beta-Lactamase Inhibitors: The Story So Far. *Curr. Med. Chem. 16*, 3740−3765.

(30) Drawz, S. M., and Bonomo, R. A. (2010) Three Decades of beta-Lactamase Inhibitors. *Clin. Microb. Rev. 23*, 160−201.

(31) Drawz, S. M., Papp-Wallace, K. M., and Bonomo, R. A. (2014) New beta-Lactamase Inhibitors: a Therapeutic Renaissance in an MDR World. *Antimicrob. Agents Chemother. 58*, 1835−1846.

(32) Bush, K., and Bradford, P. A. (2016) beta-Lactams and beta-Lactamase Inhibitors: An Overview. *Cold Spring Harbor Perspect. Med. 6*, a025247.

(33) Yang, W., Moore, I. F., Koteva, K. P., Bareich, D. C., Hughes, D. W., and Wright, G. D. (2004) TetX is a Flavin-Dependent Monooxygenase Conferring Resistance to Tetracycline Antibiotics. *J. Biol. Chem. 279*, 52346−52352.

(34) Forsberg, K. J., Patel, S., Wencewicz, T. A., and Dantas, G. (2015) The Tetracycline Destructases: A Novel Family of Tetracycline-Inactivating Enzymes. *Chem. Biol. 22*, 888−897.

(35) Volkers, G., Palm, G. J., Weiss, M. S., Wright, G. D., and Hinrichs, W. (2011) Structural Basis for a New Tetracycline Resistance Mechanism Relying on the TetX Monooxygenase. *FEBS Lett. 585*, 1061−1066.

(36) Volkers, G., Damas, J. M., Palm, G. J., Panjikar, S., Soares, C. M., and Hinrichs, W. (2013) Putative Dioxygen-Binding Sites and Recognition of Tigecycline and Minocycline in the Tetracycline-Degrading Monooxygenase TetX. *Acta Crystallogr., Sect. D: Biol. Crystallogr. D69*, 1758−1767.

(37) Park, J., Gasparrini, A. J., Reck, M. R., Symister, C. T., Elliott, J. L., Vogel, J. P., Wencewicz, T. A., Dantas, G., and Tolia, N. H. (2017) Plasticity, Dynamics, and Inhibition of Emerging Resistance Enzymes. *Nat. Chem. Biol. 13*, 730−736.

(38) van Berkel, W. J., Kamerbeek, N. M., and Fraaije, M. W. (2006) Flavoprotein Monooxygenases, a Diverse Class of Oxidative Biocatalysts. *J. Biotechnol. 124*, 670−689.

(39) Montersino, S., and van Berkel, W. J. (2013) The flavin monooxygenases. In *Handbook of Flavoproteins Vol. II: Complex Flavoproteins, Dehydrogenases and Physical Methods* (Hille, R., Miller, S., and Palfey, B., Eds.), pp 51−72, De Gruyter, Berlin, Germany. DOI: DOI: 10.1515/9783110298345.51.

(40) Huijbers, M. M. E., Montersino, S., Westphal, A. H., Tischler, D., and van Berkel, W. J. H. (2014) Flavin Dependent Monooxygenases. *Arch. Biochem. Biophys. 544*, 2−17.

(41) Romero, E., Gomez Castellanos, J. R., Gadda, G., Fraaije, M. W., and Mattevi, A. (2018) Same Substrate, Many Reactions: Oxygen Activation in Flavoenzymes. *Chem. Rev. 118*, 1742−1769.

(42) Markley, J. L., and Wencewicz, T. A. (2018) Tetracycline-Inactivating Enzymes. *Front. Microbiol. 9*, 1058.

(43) Nelson, M. L., Ismail, M. Y., McIntyre, L., Bhatia, B., Viski, P., Hawkins, P., Rennie, G., Andorsky, D., Messersmith, D., Stapleton, K., Dumornay, J., Sheahan, P., Verma, A. K., Warchol, T., and Levy, S. B.

DOI: 10.1021/acsinfecdis.8b00349
ACS Infect. Dis. XXXX, XXX, XXX−XXX

(2003) Versatile and Facile Synthesis of Diverse Semisynthetic Tetracycline Derivatives via Pd-Catalyzed Reactions. *J. Org. Chem. 68*, 5838−5851.
(44) Berens, C., Lochner, S., Lober, S., Usai, I., Schmidt, A., Drueppel, L., Hillen, W., and Gmeiner, P. (2006) Subtype Selective Tetracycline Agonists and their Application for a Two-Stage Regulatory System. *ChemBioChem 7*, 1320−1324.
(45) Berenbaum, M. C. (1978) A Method for Testing Synergy with Any Number of Agents. *J. Infect. Dis. 137*, 122−130.
(46) Luiz, M., Gutierrez, M. I., Bocco, G., and Garcia, N. A. (1993) Solvent Effect on the Reactivity of Monosubstituted Phenols Toward Singlet Molecular Oxygen in Alkaline Media. *Can. J. Chem. 71*, 1247−1252.
(47) Juretic, D., Puric, J., Kusic, H., Marin, V., and Bozic, A. L. (2014) Structural Influence on Photooxidation Degradation of Halogenated Phenols. *Water, Air, Soil Pollut. 225*, 2143.
(48) Gomez-Pacheco, C. V., Sanchez-Polo, M., Rivera-Utrilla, J., and Lopez-Penalver, J. J. (2012) Tetracycline Degradation in Aqueous Phase by Ultraviolet Radiation. *Chem. Eng. J. 187*, 89−95.
(49) Miskoski, S., Sanchez, E., Garavano, M., Lopez, M., Soltermann, A. T., and Garcia, N. A. (1998) Singlet Molecular Oxygen-mediated Photo-oxidation of Tetracyclines: Kinetics, Mechanism and Microbiological Implications. *J. Photochem. Photobiol., B 43*, 164−171.
(50) Siddens, L. K., Krueger, S. K., Henderson, M. C., and Williams, D. E. (2014) Mammalian Flavin-Containing Monooxygenase (FMO) as a Source of Hydrogen Peroxide. *Biochem. Pharmacol. 89*, 141−147.
(51) Tynes, R. E., Sabourin, P. J., Hodgson, E., and Philpot, R. M. (1986) Formation of Hydrogen Peroxide and N-Hydroxylated Amines Catalyzed by Pulmonary Flavin-Containing Monooxygenases in the Presence of Primary Alkylamines. *Arch. Biochem. Biophys. 251*, 654−664.
(52) Drug Approval Package: Tygacil (tigecycline) for Injection. U.S. Department of Health and Human Services: U.S. Food and Drug Administration. https://www.accessdata.fda.gov/drugsatfda_docs/nda/2005/21-821_Tygacil.cfm (Accessed Oct 24, 2018).
(53) Tetraphase Pharmaceuticals Announces FDA Approval of Xerava TM (Eravacycline) for Complicated Intra-Abdominal Infections (CIAI). Tetraphase Pharmaceuticals. https://ir.tphase.com/news-releases/news-release-details/tetraphase-pharmaceuticals-announces-fda-approval-xeravatm (Accessed Oct 24, 2018).
(54) News Release: Paratek Announces FDA Approval of Nuzyra™ (Omadacycline). http://investor.paratekpharm.com/phoenix.zhtml?c=253770&p=irol-newsArticle&cat=news&id=2369985 (Accessed Oct 24, 2018).
(55) Grossman, T. H., Starosta, A. L., Fyfe, C., O'Brien, W., Rothstein, D., Mikolajka, A., Wilson, D. N., and Sutcliffe, J. A. (2012) Target- and Resistance-Based Mechanistic Studies with TP-434, a Novel Fluorocycline Antibiotic. *Antimicrob. Agents Chemother. 56*, 2559−2564.
(56) Sutcliffe, J. A., O'Brien, W., Fyfe, C., and Grossman, T. H. (2013) Antibacterial Activity of Eravacycline (TP-434), a Novel Fluorocycline, against Hospital and Community Pathogens. *Antimicrob. Agents Chemother. 57*, 5548−5558.
(57) Linkevicius, M., Sandegren, L., and Andersson, D. I. (2016) Potential of Tetracycline Resistance Proteins to Evolve Tigecycline Resistance. *Antimicrob. Agents Chemother. 60*, 789−796.
(58) Michaelis, L., and Menten, M. L. (1913) Die Kinetik der Invertinwirkung. *Biochem Z. 49*, 333−369.
(59) Johnson, K. A., and Goody, R. S. (2011) The Original Michaelis Constant: Translation of the 1913 Michaelis-Menten Paper. *Biochemistry 50*, 8264−8269.
(60) Chen, W. W., Niepel, M., and Sorger, P. K. (2010) Classic and Contemporary Approaches to Modeling Biochemical Reactions. *Genes Dev. 24*, 1861−1875.

DOI: 10.1021/acsinfecdis.8b00349
ACS Infect. Dis. XXXX, XXX, XXX−XXX